1991

The added mass, Basset, and viscous drag coefficients in nondilute bubbly liquids undergoing small-amplitude oscillatory motion

Ashok S. Sangani, *Syracuse University*
D. Z. Zhang, *Johns Hopkins University*
A. Prosperetti, *Johns Hopkins University*

The added mass, Basset, and viscous drag coefficients in nondilute bubbly liquids undergoing smallamplitude oscillatory motion

A. S. Sangani, D. Z. Zhang, and A. Prosperetti

Citation: Phys. Fluids A 3, 2955 (1991); doi: 10.1063/1.857838
View online: http://dx.doi.org/10.1063/1.857838
View Table of Contents: http://pof.aip.org/resource/1/PFADEB/v3/i12
Published by the American Institute of Physics.

The added mass, Basset, and viscous drag coefficients in nondilute bubbly liquids undergoing small-amplitude oscillatory motion

A. S. Sangani
Department of Chemical Engineering and Materials Science, Syracuse University, Syracuse, New York 13244

D. Z. Zhang and A. Prosperetti
Department of Mechanical Engineering, The Johns Hopkins University, Baltimore, Maryland 21218

(Received 22 March 1991; accepted 23 August 1991)

The motion of bubbles dispersed in a liquid when a small-amplitude oscillatory motion is imposed on the mixture is examined in the limit of small frequency and viscosity. Under these conditions, for bubbles with a stress-free surface, the motion can be described in terms of added mass and viscous force coefficients. For bubbles contaminated with surface-active impurities, the introduction of a further coefficient to parametrize the Basset force is necessary. These coefficients are calculated numerically for random configurations of bubbles by solving the appropriate multibubble interaction problem exactly using a method of multipole expansion. Results obtained by averaging over several configurations are presented. Comparison of the results with those for periodic arrays of bubbles shows that these coefficients are, in general, relatively insensitive to the detailed spatial arrangement of the bubbles. On the basis of this observation, it is possible to estimate them via simple formulas derived analytically for dilute periodic arrays. The effect of surface tension and density of bubbles (or rigid particles in the case where the no-slip boundary condition is applicable) is also examined and found to be rather small.

I. INTRODUCTION

Flows involving bubbles dispersed in a liquid are important because they occur in a variety of processes. The rigorous analysis of such flows is, in general, quite complicated as the overall properties of the flow depend on the details of the microstructure of the medium (i.e., the size, shape, spatial, and velocity distribution of the bubbles) which, in turn, depend on the nature of flow. In view of the rather complex nature of the problem and its dependence on a large number of variables, such as the Reynolds number, the Weber number, the Froude number, and the volume fraction of the disperse phase, a simple theory capable of describing accurately the behavior of bubbly liquids in a wide variety of physical situations may not be possible. It is therefore desirable to devise suitable numerical simulation techniques that can be used to determine how the microstructure of the bubbly liquid evolves in various specific flow situations and how it affects the overall behavior of the bubbly liquid. It is hoped that by studying a number of different physical situations in a rigorous manner, it may be possible to develop a framework and a qualitative understanding that could be used further for modeling more complex flows.

We consider here the problem of determining the flow in a bubbly liquid produced by a small oscillatory motion imposed on it. Our motivation for studying this problem comes from the fact that it is probably the simplest situation in which the microstructure of the medium can be determined relatively easily as each bubble is simply executing a small-amplitude oscillatory motion around its mean position. Thus the spatial and size distributions of the bubbles are unaffected by the imposed oscillatory flow and the problem reduces to that of determining the velocity and deformation of bubbles given their size and spatial distribution. The situation is also of great practical significance because of its relevance to the acoustic properties of bubbly liquids.

Because of the linearity of the governing equations, in the special case of small-amplitude oscillatory motion proportional to $\exp(i\omega t)$, the mean amplitude of the bubbles' velocity is proportional to the mean amplitude of the mixture velocity and, therefore, for macroscopically homogeneous and isotropic bubbly liquids, we write

$$\langle \hat{\mathbf{v}} \rangle = \lambda_v \langle \hat{\mathbf{u}}_m \rangle, \tag{1}$$

where $\langle \hat{\mathbf{v}} \rangle$ and $\langle \hat{\mathbf{u}}_m \rangle$ denote spatial (or ensemble) averages of the amplitudes of bubble and mixture velocities, respectively, and λ_v is a constant of proportionality that depends on the frequency ω of the oscillations, the volume fraction β of the bubbles, the nondimensional surface tension σ^*, viscosity μ^*, and density ρ^* defined by

$$\sigma^* \equiv \frac{\sigma}{\rho R^3 \omega^2}, \quad \mu^* = \frac{\mu}{\rho R^2 \omega}, \quad \rho^* = \frac{\rho_b}{\rho}. \tag{2}$$

Here, R is the radius of the bubbles, all taken to be equal, and ρ is the density of the liquid.

We shall restrict our attention to the case where the frequency of oscillation ω is much smaller than the natural frequency ω_0 of the bubbles, approximately given by

$$\omega_0^2 = 3\gamma P_e/\rho R^2, \tag{3}$$

where γ is the ratio of the constant pressure and constant volume specific heats of the gas and P_e is the equilibrium pressure in the bubbles. When $\omega \ll \omega_0$, the amplitude of the

 0899-8213/91/122955-16$02.00

volume pulsations tends to zero faster than that of the translatory displacement and shape deformation so that, in examining the interactions among the bubbles, we may regard each bubble to preserve its volume as it undergoes displacement and shape oscillations.[1]

The case of small volume fraction β of gas bubbles free of surface-active contaminants has been analyzed recently by Sangani[1] using the method of pairwise interactions. His result can be expressed as

$$\lambda_v = \lambda_{v0} + \beta\lambda_{v1} + O(\beta^2). \tag{4}$$

The coefficient λ_{v0} is independent of σ^* and, for $\rho^* = 0$, it is given by

$$\lambda_{v0} = 3\left(1 - \frac{12\Omega^2 + 12\Omega^3}{1 + 3\Omega + 18\Omega^2 + 18\Omega^3}\right),$$
$$\Omega = (-i\mu^*)^{1/2}. \tag{5}$$

We note that the nondimensional viscosity, which is the inverse of the Reynolds number based on $R\omega$ as the characteristic velocity, may also be expressed in terms of ω_0 as $\mu^* = \mu/(3\gamma P_e \rho R^2 \omega_r^2)^{1/2}$, with $\omega_r = \omega/\omega_0$. For an air–water system, $\mu^* \simeq 10^{-5}/(2R\omega_r)$, R being in cm, and therefore its numerical value is small compared to unity even when ω_r is small. We shall therefore restrict our discussion to the case of small μ^* and small ω_r. More specifically, we shall be interested in the evaluation of λ_v correct to $O(\mu^*)$ and to the leading order in ω_r, i.e., to $O(\omega_r^0)$. The pairwise interaction calculations of Sangani[1] for acoustic wave propagation in dilute bubbly liquids suggest that such a limit is useful whenever ω_r is less than about 0.4. Thus the calculations for small μ^* and ω_r are, in fact, not very restricted in their applicability.

The $O(\beta)$ coefficient in (4) as a function of σ^* for $\rho^* = 0$ and small μ^* is given in Ref. 1. In particular, it was found that, for the two special cases of $\sigma^* = \infty$ and $\sigma^* = 0$, this coefficient is given by

$$\lambda_{v1} = \begin{cases} 3[-1.84 + 39.5\Omega^2 + O(\Omega^3)], & \sigma^* = \infty, \\ 3[-1.50 + 22.8\Omega^2 + O(\Omega^3)], & \sigma^* = 0. \end{cases} \tag{6}$$

For intermediate values of σ^*, the coefficient λ_{v1} does not vary smoothly between these two extreme values but rather undergoes large fluctuations whenever σ^* is less than about 0.11 owing to the shape deformation resonances that are excited by the pairwise interactions among the bubbles.[1]

The main purpose of the present study is to compute λ_v for nondilute bubbly liquids to examine how sensitive this quantity is to the details of the microstructure and the various physical properties. The results are presented for ordered as well as random dispersions of bubbly liquids. In the latter case, other statistical properties, such as the variance of the bubble velocity from its mean, are also computed. The results for λ_v can be used directly to estimate the attenuation and speed of sound waves through the use of the following relation valid for small ω_r (Ref. 1)

$$1/C_{ef}^2 = (\beta\rho/\gamma P_e)(1 - \lambda_v\beta). \tag{7}$$

Here, C_{ef} is the effective wave speed in the medium. The viscous effects make λ_v, and hence C_{ef}, a complex quantity, indicating an attenuation of sound waves. The latter can be computed from the imaginary part of the effective wave number given by the relation $k_{ef} = \omega/C_{ef}$.

Clearly, the quantity λ_v defined in (1) is related to the added mass and other forces acting on the disperse phase. We can render this connection explicit with the following arguments.

As already stated, in this paper we confine ourselves to the case of small-amplitude oscillatory motion. Under these conditions, one may write the following expression for the total force acting on a single bubble immersed in a unidirectional liquid flow at high Reynolds number,

$$\mathbf{F} = \tfrac{1}{2}\rho v_b(\dot{\mathbf{u}}_\infty - \dot{\mathbf{v}}) + 12\pi\mu R(\mathbf{u}_\infty - \mathbf{v}) + \rho v_b \dot{\mathbf{u}}_\infty. \tag{8}$$

Here, $\mathbf{v}$ is the velocity of the bubble, $v_b = 4\pi R^3/3$ is its volume, and $\mathbf{u}_\infty$ is the liquid velocity far from the bubble. The first term in the right-hand side is the added mass force, the second one is the drag at high Reynolds number, and the last one is the apparent inertia force due to the fact that the bubble partakes the motion of a liquid particle subject to the acceleration $\dot{\mathbf{u}}_\infty$. The previous expression suggests the following parametrization for the average force per bubble in the case of a mixture:

$$\langle \mathbf{F} \rangle = \tfrac{1}{2}C_a\rho v_b\langle \dot{\mathbf{u}}_m - \dot{\mathbf{v}} \rangle + \rho v_b\langle \dot{\mathbf{u}}_m \rangle + 12\pi\mu R C_d\langle \mathbf{u}_m - \mathbf{v} \rangle, \tag{9}$$

where C_a and C_d are the added mass and viscous drag coefficients normalized so that they both approach unity as $\beta \to 0$. It should be recalled that, in (9), $\mathbf{u}_m$ denotes the *mixture* velocity. Equation (9) can be expressed in terms of the average *liquid* velocity $\langle \mathbf{u} \rangle$ by using the relation

$$\langle \mathbf{u}_m \rangle = (1 - \beta)\langle \mathbf{u} \rangle + \beta\langle \mathbf{v} \rangle. \tag{10}$$

If the disperse phase can be considered massless, an exact relationship between λ_v and the coefficients C_a and C_d can be derived by simply setting the force given by (9) to zero and substituting multiplication by $i\omega$ for time differentiation. With (1), we thus find

$$\lambda_v = (2 + C_a)/C_a - 36\Omega^2(C_d/C_a^2) \quad (\rho^* = 0). \tag{11}$$

The calculation of C_a for dilute bubbly liquids has been the subject of investigations by van Wijngaarden,[2] Biesheuvel and van Wijngaarden,[3] and Biesheuvel and Spoelstra.[4] van Wijngaarden[2] determined the average velocities of the bubbles and the liquid immediately after they are set impulsively into motion and found the result

$$C_a = 1 + 2.76\beta + O(\beta^2). \tag{12}$$

He assumed the mixture to be initially at rest and the dispersion homogeneous and dilute. This result is the same as would be found by use of Eqs. (4)–(6) and (11) for $\Omega = 0$ and $\sigma^* = \infty$. This is because the average velocities of the bubbles and mixture in the situation considered by van Wijngaarden are also related by λ_v as the resulting boundary value problem is identical to the one that arises in the small-amplitude oscillatory motion examined here. Although (12) was derived for the special case of bubbly liquids initially at rest, it is also valid, as shown by Biesheuvel and Spoelstra,[4] for a situation in which an "equilibrium" flow (i.e., a uniform, steady, homogeneous flow) is given a small instantaneous velocity change. In this case, the small changes in

the average bubble and mixture velocities, $\langle \Delta \mathbf{v} \rangle$ and $\langle \Delta \mathbf{u}_m \rangle$, are once again related by the same λ_v provided that the pair probability distribution function for the spatial position of the bubbles is uniform in the equilibrium state.

Following Biesheuvel and Spoelstra, an alternative definition of the added mass coefficient can be given by imagining the actual state of motion of the dispersion generated impulsively from a state in which the liquid and particles move with the same velocity.[4,5] They calculate the increment of the liquid momentum under the action of these impulsive forces and then average over an ensemble of realizations. The added mass coefficient is obtained by division of the increment in the mean liquid momentum by the mean relative velocity between the particles and fluid. Unlike the previous definition, the added mass coefficient calculated in this way depends not only on the relative position of all the bubbles, but also on their prescribed relative velocity in the final state that is to be generated impulsively. Biesheuvel and Spoelstra assumed uniform velocity and spatial distributions and showed that, for a dilute dispersion, this alternative definition leads to a different estimate of C_a given by

$$C_a = 1 + 3.32\beta + O(\beta^2). \tag{13}$$

The reason why the two procedures for the calculation of C_a lead to different results is a consequence of the fact that the added liquid inertia depends on the distribution function of the particles' velocity. In the first case, this is determined implicitly by allowing the particles to acquire, as a consequence of the impulse, a velocity in accordance with their individual equation of motion. In the second case, the velocity distribution must be prescribed at the outset, and different choices will give different values of the numerical coefficient of the $O(\beta)$ term. When the particles in the final state all move with the same velocity, a Galilean transformation will bring them to rest. The same result (13) would then be found by computing the average force needed to keep the particles stationary when the mean liquid velocity is prescribed. This is indeed the case, as we have shown in Ref. 6.

In view of the effect of the velocity distribution on the computed value of C_a, one can expect that, for a periodic arrangement of particles, the two different approaches will give the same result. This has indeed been found by Biesheuvel and Spoelstra. It may be noted that, although the numerical results for the C_a of nondilute periodic arrays presented by these authors on the basis of their expression (35) are correct, the subsequent expression (36) that purports to give an approximate formula for the C_a of nondilute random arrays is incorrect as it suggests that this quantity will diverge as β approaches its maximum packing value.

An important question raised by the previous considerations evidently concerns the magnitude of the differences in the values of C_a that can be expected depending on the procedure used for its calculation. In this paper, we examine this point by using the first approach described above to calculate C_a, but allowing the particles' density to range from 0 to ∞. For $\rho_b = 0$, our result generalizes then van Wijngaarden's (12) to finite volume fraction. On the other hand, for $\rho_b \to \infty$, all the particles remain fixed and therefore, as noted above, we find a generalization of the result (13). Intermediate values of ρ_b will evidently be equivalent to yet other velocity distributions. Our numerical results sugget that the differences in C_a are relatively insignificant with results, in fact, not too different from those for periodic arrays. Our findings for the different ρ_b are not merely a device to examine the effect of the velocity distribution, as they can be expected to be relevant for the study of oscillatory flows of suspensions of rigid particles whenever inertial effects are of primary importance.

The expressions (12) and (13) for C_a in the case of dilute arrays were derived only for spherical bubbles. We have examined the effect of small deformation of the bubbles due to finite interfacial tension σ^*. However, in view of the fact that the shape-dependent resonance effects make λ_v a rather sensitive function of σ^* below σ^* of about 0.11, as shown by Sangani,[1] we have determined λ_v only for larger values of σ^*. For these larger values, our calculations once again show that λ_v and, hence C_a, is a rather insensitive function of σ^*.

In summary, our detailed calculations for the added mass coefficient under a variety of different conditions show it to be a rather insensitive function of most of the parameters including the detailed spatial and velocity distributions of the bubbles, density, and surface tension, suggesting thereby that the estimates of C_a as a function of β obtained here may be used in the modeling of more complex flows with a reasonable degree of confidence.

The above discussion was confined to the case of bubbles free of surface-active impurities so that boundary conditions of zero tangential stresses apply at their surface. For small bubbles, the surface-active impurities usually present affect the nature of the interface between the gas and the liquid, which can be treated as rigid. In this case, the appropriate surface boundary condition is a no-slip one and the average force is more aptly parametrized by

$$\begin{aligned}\langle \mathbf{F}(t) \rangle = {} & \rho v_b \langle \dot{\mathbf{u}}_m \rangle + \tfrac{1}{2} \rho v_b C_a \langle \dot{\mathbf{u}}_m - \dot{\mathbf{v}} \rangle \\ & + 6R^2 \sqrt{\pi \rho \mu} C_b \int_{-\infty}^{t} \langle \dot{\mathbf{u}}_m - \dot{\mathbf{v}} \rangle(\tau) \frac{d\tau}{\sqrt{t-\tau}} \\ & + 6\pi R \mu \langle \mathbf{u}_m - \mathbf{v} \rangle C_d^r. \end{aligned} \tag{14}$$

The third term in the right-hand side of this expression indicates a dependence of the force on the particle on the past history of the flow and corresponds to the Basset force (see, for example, Landau and Lifshitz[7]). For the case of oscillatory motion proportional to $\exp(i\omega t)$, the above expression can be equivalently written as

$$\begin{aligned}\langle \hat{\mathbf{F}} \rangle = {} & i\omega \rho v_b \{ \langle \hat{\mathbf{u}}_m \rangle + \tfrac{1}{2} \langle \hat{\mathbf{u}}_m - \hat{\mathbf{v}} \rangle \\ & \times [C_a + 9\Omega C_b + 9\Omega^2 C_d^r + O(\Omega^3)] \}, \end{aligned} \tag{15}$$

where carets indicate the (complex) amplitudes of the oscillating quantities. The added mass coefficient C_a, being determined from the inviscid approximation, is the same as for bubbles free of impurities. Note that the viscous correction is now large, of $O(\Omega)$, compared to the viscous correction of $O(\Omega^2)$ for impurities-free bubbles. While (14) is an exact expression for the force on an isolated sphere in a linearized Navier–Stokes flow, the expression (15) for the average

force on a bubble in a bubbly liquid has an error of $O(\Omega^3)$. The viscous drag coefficient C_d' for rigid particles is, of course, different from C_d for impurities-free bubbles. Finally, it should be noted that the averaged force on a bubble in the limit of large Ω can also be represented in terms of viscous, Basset, and added mass forces, as in (15), but the dependence of the coefficients C_d, C_b, and C_a on the volume fraction in the two cases will be quite different. The results to be presented in the present work apply only for small Ω.

The analysis for the determination of the viscous corrections to λ_v by properly taking into account the presence of a Stokes layer on the surface of each impurities-free bubble as presented by Sangani[1] is modified here to treat the case of a no-slip boundary condition. Although the thickness of the Stokes layer is small, the viscous corrections cannot be determined directly from an application of the usual boundary layer type of analysis for flat surfaces because displacement thickness effects are important. It is convenient instead to use expansions for the velocity field in terms of Legendre polynomials around the center of each bubble. An interesting result of the analysis for the no-slip particles is that, if the angular velocity is expanded in powers of Ω, the coefficient of each term is identically zero, indicating thereby that the mean angular velocity of rigid particles placed in a simple oscillatory flow must approach zero faster than any power of Ω as $\Omega \to 0$.

The calculations of the first viscous effects, i.e., the determination of C_b for rigid particles and C_d for impurities-free bubbles, involve similar boundary value problems and, in fact, it can be shown that C_b for massless particles is exactly the same as C_d for impurities-free bubbles with $\sigma^* = \infty$ and $p^* = 0$. Our detailed numerical calculations for nondilute periodic and random arrangements of bubbles show, once again, that these coefficients are relatively insensitive to the details of the spatial distribution of the bubbles. The drag coefficient C_d' for no-slip particles, on the other hand, appears to be somewhat sensitive to the spatial distribution for higher values of β.

Finally, we also present calculations for the analytical determination of the various force coefficients for dilute periodic and random arrays. The expressions for the periodic arrays are correct to $O(\beta^{10/3})$ and, in the light of the finding that the various force coefficients are insensitive to the spatial distributions of the bubbles, serve as useful simple formulas that could be used in modeling more complex flows of bubbly liquids in which the inertial effects are of primary importance and in which the bubbles remain approximately spherical. In particular, it is found that the asymptotic formula for C_a for dilute periodic arrays gives predictions that are within 5% of the computed values for random and body-centered cubic arrays for $0 \leqslant \beta \leqslant 0.5$. An analysis is also presented for the mean-squared fluctuation or variance of the amplitude of the bubble velocity from its mean. Such calculations are expected to be useful in investigations of the stability of homogeneous flows of bubbly liquids when subjected to small nonuniform perturbations in β.

The organization of the paper is as follows. In Sec. II, we present the method to determine the viscous corrections. The interaction between all the particles is essentially the same as in potential flow: The consideration of thin Stokes layers near the surface of each particle only modifies the boundary condition to be satisfied by the potential flow approximation. In Sec. III, we present analyses for dilute periodic and random arrays. Only the case of rigid surfaces is treated in detail as this represents a significant modification from the previous work of Sangani.[1] Section IV addresses the relationship between the added mass coefficient and the effective thermal or electrical conductivity of a composite consisting of spheres in a matrix. Numerical results are presented in Sec. V.

II. FORMULATION OF THE PROBLEM AND THE METHOD OF ANALYSIS

For numerical simulations of many-bubble interactions in a random dispersion that is homogeneous and infinitely extended, we have recourse to a widely used artifice consisting in, first, randomly placing N bubbles in a cubic cell and then filling up the entire space with copies of this cell. The desired quantities, such as λ_v, are calculated for this configuration of the dispersion and the process is then repeated for several different configurations of the N bubbles in the basic cell until the averages of the quantities over a number of configurations do not change appreciably. Actually, such configurations need not be isotropic, and hence λ_v is a tensor of rank two. For sufficiently large N, however, the off-diagonal elements of the tensor are generally small and a scalar estimate of λ_v can be obtained by taking the average of the three diagonal components of the tensor. The calculations are then repeated for larger N until the averaged quantities as a function of N do not change significantly either. Thus the problem reduces to determining the velocity field when the positions of N bubbles within the basic unit cell are specified.

We shall assume that the liquid may be regarded as incompressible and Newtonian and that the magnitude of the velocity is small everywhere. When the nonlinear and gravity terms in the equations of motion are negligible, the velocity field in the fluid is governed by the following equations:

$$\nabla \cdot \mathbf{u} = 0, \tag{16}$$

$$\rho \frac{\partial \mathbf{u}}{\partial t} = -\nabla p + \mu \nabla^2 \mathbf{u}. \tag{17}$$

We shall assume that the velocity and pressure vary sinusoidally with time as $\exp(i\omega t)$ with the corresponding amplitudes denoted by a caret. The solution of the above equations can be expressed in terms of three scalar functions (see Kim and Russel[8]):

$$\hat{\mathbf{u}} = -\nabla P + \sum_{\alpha} \{\nabla \times \nabla \times [(\mathbf{x} - \mathbf{x}^{\alpha})\Phi^{\alpha}] + \nabla \times [(\mathbf{x} - \mathbf{x}^{\alpha})\chi^{\alpha}]\}, \tag{18}$$

where $\mathbf{x}^{\alpha}$ is the position vector of the center of the bubble α, $P = \hat{p}/(i\omega\rho)$, and Φ^{α} and χ^{α} are, respectively, the toroidal and poloidal fields due to the bubble α. The summation is taken over all the bubbles in the dispersion. The functions P, Φ^{α}, and χ^{α} satisfy the following equations:

$$\nabla^2 P = 0, \quad \Omega^2 R^2 \nabla^2 \Phi^{\alpha} = \Phi^{\alpha}, \quad \Omega^2 R^2 \nabla^2 \chi^{\alpha} = \chi^{\alpha}, \tag{19}$$

where Ω is defined in (5). These functions are to be deter-

mined from the boundary conditions on the surface of each bubble. For this purpose, it is convenient to express them in a series of spherical harmonics. Thus, in a polar coordinate system (r,θ,ϕ) centered at the center of the bubble α, we express P in the neighborhood of that bubble as

$$P = \sum_{n=0}^{\infty} \sum_{m=0}^{n} [P_{nm}^{\alpha}(r) \cos m\phi + \tilde{P}_{nm}^{\alpha}(r) \sin m\phi] \times P_n^m(\cos\theta), \tag{20}$$

where

$$P_{nm}^{\alpha} = C_{nm}^{\alpha} r^n + E_{nm}^{\alpha} r^{-n-1}, \tag{21}$$

with a similar expression for $\tilde{P}_{nm}^{\alpha}$. We are interested in the case of small Ω, for which it can easily be seen that Φ^{α} and χ^{α} decay to zero exponentially within a distance $O(\Omega R)$ from the surface of the bubble α. Thus the poloidal and toroidal fields of a bubble γ, $(\gamma \neq \alpha)$, will have a vanishing contribution to the velocity field around the surface of the bubble α, provided that ΩR is small compared to the minimum distance between the surface of the two bubbles, which we shall assume to be the case. In a random configuration of bubbles there is, of course, a finite probability that two bubbles will be close enough for their Stokes layers to overlap, but it will be shown that the inclusion of overlapping Stokes layer is necessary only in determining corrections to orders higher than Ω^2 [cf. the discussion following (74)]. The pressure, on the other hand, varies on length scales comparable to the radius of the bubbles and their separation distances, and thus its computation requires that interactions among all the bubbles be accounted for. The scheme for solving this problem therefore consists of two steps. In the first step, we determine the condition satisfied by the pressure at the surface of a bubble by taking into account the presence of the adjacent Stokes layer and then, in the second step, we ignore the Stokes layer in the vicinity of each bubble and determine the pressure by solving the appropriate multiparticle interaction problem with the boundary conditions at the surface of the bubbles derived from the first step.

We now consider the first step, i.e., the determination of the boundary conditions for P_{nm}^{α} and $\tilde{P}_{nm}^{\alpha}$ at $r = R$, the surface of the generic bubble. Ignoring the exponentially decaying poloidal and toroidal fields due to other bubbles, the velocity field near a bubble can be written as

$$\hat{u}_r = -\frac{\partial P}{\partial r} - r\nabla_s^2 \Phi, \tag{22}$$

$$\hat{u}_\theta = -\frac{1}{r}\frac{\partial}{\partial \theta}\left(P - \frac{\partial}{\partial r}(r\Phi)\right) + \frac{1}{r\sin\theta}\frac{\partial \chi}{\partial \phi}, \tag{23}$$

$$\hat{u}_\phi = \frac{1}{r\sin\theta}\frac{\partial}{\partial \phi}\left(P - \frac{\partial}{\partial r}(r\Phi)\right) - \frac{1}{r}\frac{\partial \chi}{\partial \theta}, \tag{24}$$

where, for brevity, we have dropped the superscript α on Φ and χ, and ∇_s^2 is the surface Laplacian, i.e., the Laplacian operator in spherical coordinates without the radial derivatives. The components of the force and torque acting on the bubble can be shown to be given by

$$\hat{F}_1 = (4\pi R^2/3) i\omega\rho(2\Phi_{10} - P_{10}),$$
$$\hat{F}_2 = (4\pi R^2/3) i\omega\rho(P_{11} - 2\Phi_{11}), \tag{25}$$

$$\hat{\mathscr{L}}_1 = \frac{8\pi R^3}{3}\mu D\left(\frac{\chi_{10}}{r^2}\right), \quad \hat{\mathscr{L}}_2 = \frac{8\pi R^3}{3}\mu D\left(\frac{\chi_{11}}{r^2}\right), \tag{26}$$

with the expressions for $\hat{F}_3$ and $\hat{\mathscr{L}}_3$ similar to those for $\hat{F}_2$ and $\hat{\mathscr{L}}_2$ with P_{nm}, Φ_{nm}, and χ_{nm} replaced by $\tilde{P}_{nm}$, $\tilde{\Phi}_{nm}$, and $\tilde{\chi}_{nm}$, respectively. Here, $\Phi_{nm}(r)$, $\chi_{nm}(r)$, etc., are the coefficients of the expansions of Φ and χ in Legendre polynomials analogous to (20). In the above expressions, $D(\cdot) \equiv R d(\cdot)/dr$, and all of the quantities are to be evaluated at the surface of the bubble α, i.e., at $r = R$.

We shall consider separately the two cases of boundary conditions at the interface mentioned previously.

A. No-slip boundary condition

The first case is that of rigid spheres for which the no-slip boundary condition applies at the surface. As mentioned in the Introduction, this case is appropriate for surface-contaminated small bubbles for which the molecules of impurities form a tight monolayer over the entire surface of the bubble. This case is also applicable to rigid particles and, for the sake of generality, we shall therefore take ρ_b, the density of the particles, to be finite. It may be noted that, unlike the more usual situation of boundary layers on bluff objects, the Stokes layer remains attached to the surface of the particle due to the linearization approximation.

The velocity on the bubble surface is given by

$$\hat{\mathbf{u}} = \hat{\mathbf{v}} + \hat{\mathbf{w}} \times \mathbf{r}, \quad \text{at } r = R. \tag{27}$$

The amplitudes of the translational $\hat{\mathbf{v}}$ and rotational $\hat{\mathbf{w}}$ speeds of the particle are to be determined as part of the solution from the two additional equations

$$\hat{\mathbf{F}} = \rho_b v_b i\omega\hat{\mathbf{v}}, \quad \hat{\mathscr{L}} = \tfrac{2}{3}\rho_b v_b R^2 i\omega\hat{\mathbf{w}}, \tag{28}$$

with $\hat{\mathbf{F}}$ and $\hat{\mathscr{L}}$ the force and torque given by (25) and (26). The unknowns $\hat{\mathbf{v}}$ and $\hat{\mathbf{w}}$ are also related to P_{1m}, Φ_{1m}, etc., through the kinematic boundary condition. For example, it can be shown that

$$R\hat{v}_1 = -D(P_{10}) + 2\Phi_{10} = (1/R)[D(r\Phi_{10}) - RP_{10}], \tag{29}$$

$$R^2\hat{w}_1 = \chi_{10}. \tag{30}$$

Now we expand P_{nm}, Φ_{nm}, and χ_{nm} in a series of powers of Ω. Thus, for example, we write

$$P_{nm}(r) = \sum_{s=0}^{\infty} P_{nm}^s(r)\Omega^s \tag{31}$$

and solve for the coefficients P_{nm}^s, etc., by comparing the coefficients of $O(\Omega^s)$ in the governing equations. Since Φ and χ satisfy (19), the functions Φ_{nm}^s and χ_{nm}^s are proportional to the modified spherical Bessel functions k_n that, for small Ω, are proportional to $\exp[-(r-R)/(\Omega R)]/r$. Thus the radial derivatives of Φ and χ are much greater than the values of these functions at $r = R$. From (26), (28), and (30), we then see that the angular momentum condition is satisfied only if $\chi_{10}^s = 0$ for all s. The same result applies to the other two components of the angular velocity, and thus we deduce that $\hat{\mathbf{w}} \to 0$ as $\Omega \to 0$ faster than any algebraic power of Ω. As a consequence, the toroidal field χ vanishes and the problem reduces to determining the relation between

Φ and P. Now, the no-slip boundary condition for the angular components of the velocity is satisfied by choosing

$$RP_{nm} - D(r\Phi_{nm}) = 0, \quad n \geqslant 2, \quad r = R, \tag{32}$$

and substitution for Φ_{nm} in the no-slip condition for the radial component of the velocity yields another relation between these functions,

$$D(P_{nm}) = n(n+1)\Phi_{nm}, \quad n \geqslant 2, \quad r = R. \tag{33}$$

To eliminate Φ_{nm} from the above two equations, we make use of the fact that Φ_{nm}, being proportional to the modified spherical Bessel function k_n, near $r = R$ behaves as

$$[D(r\Phi_{nm})]_{r=R} = -\{1/\Omega + [n(n+1)/2]\Omega + O(\Omega^2)\}\Phi_{nm}(R). \tag{34}$$

From (32)–(34), we see that Φ_{nm} is $O(\Omega)$ and, upon solving for the first three corrections, we find

$$D(P_{nm}) = -n(n+1)\Omega P_{nm}, \quad n \geqslant 2, \quad r = R, \tag{35}$$

correct to $O(\Omega^2)$. These equations are also satisfied by $\tilde{P}_{nm}$. The conditions for $n = 1$, i.e., for P^s_{1m} at $r = R$, are obtained next by combining the no-slip and the force balance conditions and solving the resulting equations for each power in Ω separately. The results of the analysis up to $O(\Omega^2)$ can then be recast in the following compact forms:

$$\Phi_{1m} = (\Omega - 2\Omega^2)[D(P_{1m}) - P_{1m}], \quad r = R, \tag{36}$$

$$P_{1m} - \rho^* D(P_{1m}) = 2(1-\rho^*)\Phi_{1m} = 2(1-\rho^*)\Omega(1-2\Omega)[D(P_{1m}) - P_{1m}], \tag{37}$$

where $\rho^* = \rho_b/\rho$. Finally, the velocity of the particle can be calculated to $O(\Omega^2)$ from

$$R\hat{v}_1 = -D(P_{10}) + 2\Phi_{10} = [P_{10} - D(P_{10})]/(1-\rho^*). \tag{38}$$

The expressions for $-\hat{v}_2$ and $-\hat{v}_3$ can be obtained by replacing P_{10} in the above expression by, respectively, P_{11} and $\tilde{P}_{11}$.

Equations (35) and (37) represent the boundary conditions for the pressure coefficients at the surface of the rigid particles obtained by accounting for the pressure interaction among the particles while neglecting the viscous interaction. Note that the quantities in the right-hand sides are multiplied by Ω and therefore P^s_{nm}, the coefficient of the Ω^s term in the expansion (31) of $P_{nm}(r)$, can be calculated by successive approximations for s up to 2.

B. Free-slip boundary conditions

This case is more suitable for larger, but approximately spherical, bubbles or bubbles in liquids less prone to amphiphilic contamination than water. Now the boundary conditions are the usual kinematic and dynamic conditions at a free-slip surface. For the present analysis, we shall take the density of the bubbles to be zero, but we will allow them to deform. The poloidal field Φ is now $O(\Omega^2)$ and, unlike the previous case, the toroidal field is not exponentially small in Ω, but rather $O(\Omega^3)$. Appropriate forms of the boundary conditions valid to $O(\Omega^2)$ have been derived by Sangani,[1] and are

$$\Phi_{nm} = 2\Omega^2[D(P_{nm}) - P_{nm}], \tag{39}$$

$$P_{nm} + (n-1)(n+2)\sigma^* D(P_{nm}) = -2\Omega^2\{D^2(P_{nm}) + n(n^2-1)(n+2)\sigma^*[P_{nm} - D(P_{nm})]\}, \tag{40}$$

where $\sigma^* = \sigma/(\rho\omega^2 R^3)$ denotes the nondimensional interfacial tension. The velocity component in the x_1 direction in this case is given by

$$R\hat{v}_1 = -D(P_{10}) + 2\Phi_{10} = -(1-4\Omega^2)D(P_{10}), \tag{41}$$

where we have made use of the fact that $P^0_{10} = 0$ at $r = R$ since the surface tension term in (40) vanishes for $n = 1$.

It may be noted that there is a relationship between the problems of determining P^1_{nm} of rigid particles with $\rho^* = 0$ and for P^2_{nm} of impurities-free bubbles with $\sigma^* = \infty$. For large surface tension, the term involving two derivatives of P_{nm} in (40) can be neglected for $n \geqslant 2$ and, from (21), we find that $D(P_{1m}) - P_{1m} = -3E_{1m}R^{-2} = -D^2(P_{1m})/2$. Consequently, comparing the two problems, we see that P^2_{nm} for impurities-free bubbles with $\sigma^* = \infty$ is exactly twice P^1_{nm} of rigid particles with $\rho^* = 0$. This observation subsequently yields $C_b(\rho^* = 0) = C_d(\sigma^* = \infty)$.

C. The multibubble interaction calculations for the pressure

Having derived the appropriate boundary conditions for P_{nm} at the surface of each bubble for the above two special cases, the next step is to incorporate them into the multibubble interactions. The procedure for this is similar to the one described in Sangani and Yao.[9] Briefly, since P satisfies the Laplace equation, and since the problem of N randomly placed bubbles in the basic unit cell repeated throughout the entire space is equivalent to a superposition of N randomly placed periodic lattices, we express P in terms of periodic singular solutions of the Laplace equation[10] as

$$P(\tilde{x}) = -\mathbf{G}\cdot\mathbf{x} + \sum_{\alpha=1}^{N}\sum_{n=1}^{\infty}\sum_{m=0}^{m=n} 2^{m-1}\partial_1^{n-m}(A^{\alpha}_{nm}\Delta_m + \tilde{A}^{\alpha}_{nm}\tilde{\Delta}_m)S_1(\mathbf{x}-\mathbf{x}^{\alpha}), \tag{42}$$

where $\partial_1 \equiv \partial/\partial x_1$, $\mathbf{x}^{\alpha}$ denotes the position of the center of the bubble α in the basic unit cell,

$$\Delta_m = \left(\frac{\partial}{\partial\xi}\right)^m + \left(\frac{\partial}{\partial\eta}\right)^m,$$

$$\tilde{\Delta}_m = i\left[\left(\frac{\partial}{\partial\xi}\right)^m - \left(\frac{\partial}{\partial\eta}\right)^m\right], \tag{43}$$

$$\xi = x_2 + ix_3, \quad \eta = x_2 - ix_3, \tag{44}$$

and S_1 is defined in Ref. 10. In the low-frequency acoustic application we are considering here, the wavelength of sound is large compared with the size of the basic cell and it is therefore appropriate to approximate the mean pressure field by a linear variation with position. For this reason, in the above expression for P, we have assumed that there exists

a mean gradient $\mathbf{G}$. It should be noted that Eq. (42), as written, is exact and is equivalent to a simultaneous multipole expansion around each bubble.

To determine the unknown coefficients A^{α}_{nm} and $\tilde{A}^{\alpha}_{nm}$ in (42) from the boundary conditions on the surface of the bubbles, we equate the representation (42) with the representations (20) valid in the neighborhood of each bubble. It is found[9] that the coefficient E^{α}_{nm} appearing in the expression (21) for P^{α}_{nm} is related to A^{α}_{nm} by

$$E^{\alpha}_{nm} = (-1)^{n-m}(n-m)!A^{\alpha}_{nm}, \tag{45}$$

with a similar expression for $\tilde{E}^{\alpha}_{nm}$ and $\tilde{A}^{\alpha}_{nm}$. Similarly, from Ref. 9,

$$C^{\alpha}_{nm} = [(-2)^m/(1+\delta_{m0})] \times [1/(n+m)!](\partial_1^{n-m}\Delta_m P^{(r)})_{\mathbf{x}=\mathbf{x}^{\alpha}}, \tag{46}$$

where $P^{(r)}$ is the part of P regular in the neighborhood of $\mathbf{x}^{\alpha}$, i.e.,

$$P^{(r)} = -\mathbf{G}\cdot\mathbf{x} + \sum_{\gamma=1}^{N}\sum_{k=1}^{\infty}\sum_{j=0}^{k} 2^{j-1}(A^{\gamma}_{kj}\Delta_j + \tilde{A}^{\gamma}_{kj}\tilde{\Delta}_j) \times \partial_1^{k-j}\left(S_1(\mathbf{x}-\mathbf{x}^{\gamma}) - \frac{\delta_{\gamma\alpha}}{|\mathbf{x}-\mathbf{x}^{\alpha}|}\right). \tag{47}$$

A method for the efficient evaluation of the derivatives of S_1 appearing in this equation is described in the Appendix. The following step is to expand A^{α}_{nm}, etc., in a series in powers of Ω and, using the boundary conditions on P_{nm}, obtain the relations among the coefficients $C^{s,\alpha}_{nm}$ and $E^{s,\alpha}_{nm}$ of $O(\Omega^s)$ with $s=0$, 1, and 2. The resulting set of equations is linear and can be solved after truncation to a finite number of equations containing A_{nm} and $\tilde{A}_{nm}$ with $n \leqslant N_s$ in (42). The translational velocity of each bubble is evaluated by making use of relations (38) and (41). The calculations are then repeated for larger values of N_s until the results converge. To calculate λ_v, we also need to evaluate the average velocity of the mixture. This is described next.

D. The average velocity of the mixture

To determine the average velocity of the mixture, we need to evaluate the integral of the velocity field over the volume occupied by the liquid within the basic unit cell. Let us decompose the velocity in two components, $\hat{\mathbf{u}} = \hat{\mathbf{u}}^P + \hat{\mathbf{u}}^{\Phi}$ with $\hat{\mathbf{u}}^P = -\nabla P$ and $\hat{\mathbf{u}}^{\Phi} = \Sigma\nabla\times\nabla\times[(\mathbf{x}-\mathbf{x}^{\alpha})\Phi^{\alpha}]$. The integral of $\hat{\mathbf{u}}^P$ over the liquid volume can be shown to be

$$\int_{V_L}\hat{\mathbf{u}}^P\,dV = \mathbf{G}V + \sum_{\alpha=1}^{N}\int_{S^{\alpha}} P\mathbf{n}\,dA, \tag{48}$$

where V_L is the volume occupied by the liquid, V is the volume of the basic cell, S^{α} is the surface of the bubble α, and $\mathbf{n}$ is the unit outward normal at the surface of the bubble. The surface integral in (48) can be related to P_{1m} and thus the contribution to the average velocity due to this part can be readily evaluated. Next, we note that the contribution due to Φ^{α} is important only near the surface of the bubble α. The Stokes layer is $O(\Omega R)$ and the tangential velocity contribution due to Φ^{α} in this layer is $O(1)$. Thus the integral of $\hat{\mathbf{u}}^{\Phi}$ contributes an $O(\Omega)$ quantity in the case of bubbles with a rigid interface. The corresponding contribution for the case of impurities-free bubbles is $O(\Omega^2)$ as the tangential velocity correction in this case is $O(\Omega)$, the Stokes layer being $O(R\Omega)$ thick in both cases. The contribution due to this poloidal field near the bubble α can be shown to be

$$\int\hat{u}_1^{\Phi}\,dV = 2\pi\int_R^{\infty}\int_0^{\pi}\left(\frac{d}{dr}(r\Phi^{\alpha}_{10})\sin^2\theta + 2\Phi^{\alpha}_{10}\cos^2\theta\right) \times r\sin\theta\,d\theta\,dr = -\frac{8\pi R^2}{3}\Phi^{\alpha}_{10}. \tag{49}$$

Combining now the contributions from both parts, we obtain

$$\int_{V_L}\hat{u}_1\,dV = G_1 V + \frac{v_b}{R}\sum_{\alpha=1}^{N}(P^{\alpha}_{10} - 2\Phi^{\alpha}_{10}) + O(\Omega^3). \tag{50}$$

On using (36)–(38), it can be shown further that $P^{\alpha}_{10} - 2\Phi^{\alpha}_{10} = -\rho^* R\hat{v}^{\alpha}_1$.

Since the average velocity inside the bubble α is $\hat{\mathbf{v}}^{\alpha}$, the average mixture velocity can now be evaluated from

$$\langle\hat{\mathbf{u}}_m\rangle = \mathbf{G} + \beta(1-\rho^*)\langle\hat{\mathbf{v}}\rangle. \tag{51}$$

This result, with $\rho^* = 0$, also applies to the case of impurities-free bubbles.

III. SPECIAL CASES

Before presenting the results for nondilute bubbly mixtures, let us examine a few special cases. The simplest one is, of course, that of an isolated bubble. If we take $G_i = \delta_{i1}$, then only P_{10} is nonzero and we can write

$$P_{10}(r) = -r + A_{10}/r^2. \tag{52}$$

For the no-slip boundary condition case, the successive approximations satisfy [cf. (37)], at $r=R$,

$$\begin{aligned} &P^0_{10} - \rho^* D(P^0_{10}) = 0,\\ &P^1_{10} - \rho^* D(P^1_{10}) = 2(1-\rho^*)[D(P^0_{10}) - P^0_{10}],\\ &P^2_{10} - \rho^* D(P^2_{10}) = 2(1-\rho^*)\{[D(P^1_{10}) - P^1_{10}] - 2[D(P^0_{10}) - P^0_{10}]\}, \end{aligned} \tag{53}$$

whereby A_{10} can be readily evaluated to be

$$\frac{A_{10}}{R^3} = \frac{1-\rho^*}{1+2\rho^*}\left(1 - 6\Omega\frac{1-\rho^*}{1+2\rho^*} + 12\Omega^2\frac{(4-\rho^*)(1-\rho^*)}{(1+2\rho^*)^2}\right). \tag{54}$$

Actually, the $O(\Omega^3)$ and all of the subsequent corrections vanish identically, so that (54) is an exact result for an isolated sphere. Now, λ_v for an isolated rigid particle can be readily evaluated to be

$$\lambda_v = \frac{3}{1+2\rho^*}\left(1 - 6\Omega\frac{1-\rho^*}{1+2\rho^*} + 12\Omega^2\frac{(4-\rho^*)(1-\rho^*)}{(1+2\rho^*)^2}\right). \tag{55}$$

Setting $\hat{\mathbf{F}} = \rho_b i\omega v_b\lambda_v\hat{\mathbf{u}}_m$ in (15), we see that the above expression for an isolated rigid sphere agrees with (15) if we take $C_a = C_b = C^r_d = 1$.

Similarly, the calculation of λ_v for an isolated impurities-free bubble with $\rho^* = 0$ gives

$$\lambda_v = 3[1 - 12\Omega^2 + O(\Omega^3)]. \tag{56}$$

This result is in agreement with (11) if we take $C_a = C_d = 1$.

A. Dilute periodic arrays

Let us now obtain results for dilute cubic periodic arrays. In this case, the basic cell contains only one bubble so that $N = 1$ and Eq. (42) for P is

$$P = -x_1 + A_{10}\frac{\partial S_1}{\partial x_1} + A_{20}\frac{\partial^3 S_1}{\partial x_1^3} + \cdots. \tag{57}$$

It can be shown that A_{20} contributes to λ_v only at $O(\beta^{10/3})$ and, therefore, we need only retain A_{10} to determine the first few approximations to λ_v. Now, S_1 can be expanded near the center of a bubble in the basic unit cell as[10]

$$S_1 = 1/r - c + 2\pi r^2/3V + O(r^4), \tag{58}$$

where c is a constant that depends on the geometry. Since we are presently interested only in the derivatives of S_1, the magnitude of this constant is not important. Thus P_{10} can be approximated now by

$$P_{10} = r[-1 + \beta(A_{10}/R^3) + O(\beta^{10/3})] - A_{10}/r^2. \tag{59}$$

Substituting for P_{10} in (53), solving for A_{10} to $O(\Omega^2)$, and determining the velocity of bubbles and mixture from (38) and (51), we obtain the following estimate of λ_v for the special case $\rho^* = 0$:

$$\lambda_v = 3/[1 + 2\beta + 6\Omega(1 - 2\Omega)] + O(\Omega^3, \beta^{10/3}). \tag{60}$$

This result can be alternatively expressed in terms of a force coefficient C defined, on the basis of (15), via

$$C \equiv C_a + 9\Omega C_b + \Omega^2 C_d' + O(\Omega^3) = 2(\rho^*\lambda_v - 1)/(1 - \lambda_v). \tag{61}$$

Thus, upon substituting (60) into (61) and taking $\rho^* = 0$, we obtain

$$C = \frac{1 + 2\beta + 6\Omega(1 - 2\Omega)}{1 - \beta - 3\Omega(1 - 2\Omega)} = \frac{1 + 2\beta}{1 - \beta} + 9\Omega\frac{1}{(1 - \beta)^2} + 9\Omega^2\frac{1 + 2\beta}{(1 - \beta)^3} + O(\beta^{10/3}, \Omega^3). \tag{62}$$

Although the above expression for C, which can readily be related to C_a, C_b, and C_d' via (61), is derived here for the special case of $\rho^* = 0$, it can be shown that the result is actually valid for arbitrary ρ^*. The result for the added mass coefficient, i.e.,

$$C_a = (1 + 2\beta)/(1 - \beta) + O(\beta^{10/3}), \tag{63}$$

agrees with the widely used expression first given by Zuber[11] who derived it using a cell model, which is thus exact for periodic arrays to $O(\beta^{10/3})$.

The above results for C apply to periodic arrays of rigid particles. For bubbles free of surface-active impurities, it can similarly be shown that

$$C \equiv C_a + 18\Omega^2 C_d + O(\Omega^3) = (1 + 2\beta)/(1 - \beta) + 18[\Omega^2/(1 - \beta)^2] + O(\beta^{10/3}). \tag{64}$$

This result is independent of surface tension, which only affects the boundary conditions for P_{nm} with $n \geqslant 2$. The consideration of this parameter is therefore only important in the calculation of terms of order $O(\beta^{10/3})$ and higher.

B. Dilute random arrays

Let us now determine the $O(\beta)$ correction to C for dilute random arrays. The procedure for calculating this correction from the pairwise interaction of particles is now well established. In principle, it consists of determining the velocity of a particle (referred to as the test particle) placed at, say, the origin, in the presence of a second particle situated at $\mathbf{S}$ and then multiplying it by the probability of finding the particle at $\mathbf{S}$ and integrating over all possible values of $\mathbf{S}$. Since the disturbance created by the second particle modifies the velocity of the test particle by an amount proportional to $(R/S)^3$ for large S, this direct method of calculating the $O(\beta)$ correction leads to a nonabsolutely convergent integral. Methods to overcome such difficulties have been described in the literature (see, for example, Refs. 12–15). Following Hinch's method, we split the calculation of the average velocity of the test particle into two parts and write

$$\langle \hat{\mathbf{v}} \rangle = \langle \hat{\mathbf{v}}_e \rangle + \langle \hat{\mathbf{v}}_p \rangle, \tag{65}$$

where $\langle \hat{\mathbf{v}}_p \rangle$ represents the contribution from pairwise interactions and $\langle \hat{\mathbf{v}}_e \rangle$ corresponds to the velocity of the particle placed in an effective medium with a uniform distribution of dipoles (see Sangani[1]). The strength of these dipoles is the same as the dipole induced in an isolated particle and is related to A_{10} given by (54). Thus $\langle \hat{\mathbf{v}}_e \rangle$ can be shown to be given by

$$\langle \hat{\mathbf{v}}_e \rangle = \lambda_{v0}(1 + \beta A_{10} R^{-3})\mathbf{G}, \tag{66}$$

where $\mathbf{G}$ is the value of $-\nabla P$ at infinity and A_{10} and λ_{v0}, the coefficient of $O(\beta^0)$ in λ_v, are given by (54) and (55), respectively. The quantity $\mathbf{G}$ can be related to the average velocity of the mixture from the ensemble-averaged momentum equation by

$$\langle \hat{\mathbf{u}}_m \rangle = [1 + \beta\lambda_{v0}(1 - \rho^*)]\mathbf{G}. \tag{67}$$

The part $\langle \hat{\mathbf{v}}_p \rangle$ corresponds to the contribution from pairwise interactions and can be written as

$$\langle \hat{\mathbf{v}}_p \rangle = \int_{S>2R} \hat{\mathbf{v}}^*(\mathbf{O}|\mathbf{S}) P(\mathbf{S}|\mathbf{O}) dV, \tag{68}$$

where $P(\mathbf{S}|\mathbf{O})$ is the probability of finding a particle at a separation vector $\mathbf{S}$ from the test particle and $\hat{\mathbf{v}}^*(\mathbf{O}|\mathbf{S})$ is the velocity of the test particle in the presence of the second particle minus the first two reflections of $O[(R/S)^0]$ and $O[(R/S)^3]$ in the interaction of the two particles. The reason for subtracting these reflections is that the calculation of $\langle \hat{\mathbf{v}}_e \rangle$ already accounts for them (see Sangani[1] and Acrivos and Chang[14]). Now, because of the linearity of the governing equations, we can write

$$\hat{\mathbf{v}}^*(\mathbf{O}|\mathbf{S}) = g_{11}\mathbf{G} + (g_{01} - g_{11})[(\mathbf{G}\cdot\mathbf{SS})/S^2], \quad (69)$$

where g_{01} and g_{11} are scalar functions of S/R to be determined by solving separately two problems with the separation vector between the two spheres aligned parallel and perpendicular to $\mathbf{G}$. Both functions decay to zero as $(R/S)^6$ as $S \to \infty$. The force coefficient C, given by [cf. (61)]

$$C = 2\frac{\rho^*\langle\hat{v}\rangle - \langle\hat{u}_m\rangle}{\langle\hat{u}_m\rangle - \langle\hat{v}\rangle}, \quad (70)$$

can now be determined correct to $O(\beta)$ by substituting for $\langle\hat{\mathbf{v}}\rangle$ and $\langle\hat{\mathbf{u}}_m\rangle$ from (65)–(69) to find

$$C = C_0 + \frac{1}{3}\beta(2 + C_0)^2 - \frac{C_0 + 2\rho^*}{2(1-\rho^*)}\frac{\langle\hat{v}_p\rangle}{G}, \quad (71)$$

where $C_0 \equiv 1 + 9\Omega + 9\Omega^2$ is the $O(\beta^0)$ term in C. In writing (70) and (71), we have used the fact that, due to the isotropy of the pair probability distribution function $P(\mathbf{S}|\mathbf{O})$, $\langle\hat{\mathbf{u}}_m\rangle$, $\langle\hat{\mathbf{v}}_p\rangle$, and $\langle\hat{\mathbf{v}}\rangle$ are all parallel to $\mathbf{G}$.

We note that, for periodic arrays $P(\mathbf{S}|\mathbf{O}) = 0$ for $S/R < O(\beta^{1/3})$ so that $\langle\hat{\mathbf{v}}_p\rangle = 0$ and the above result (71) agrees with that derived in the previous subsection [cf. (62)] to $O(\beta)$. In fact, the result for periodic arrays is correct to $O(\beta)$ for all well-separated random arrays, i.e., arrays in which $P(\mathbf{S}|\mathbf{O}) = 0$ for $S = O(R)$.

For well-stirred random arrays of nonoverlapping spheres, we take $P(\mathbf{S}|\mathbf{O}) = \beta/v_b$ $(S > 2R)$ and, upon substituting $C_0 = 1 + 9\Omega + 9\Omega^2$ in (71) and making use of (69), we obtain

$$\begin{aligned} C &= C_a + 9\Omega C_b + 9\Omega^2 C_d^r \\ &= 1 + 9\Omega + 9\Omega^2 + 3\beta(1 + 6\Omega + 15\Omega^2) \\ &\quad - \frac{C_0 + 2\rho^*}{2(1-\rho^*)}\frac{\beta}{R^3}\int_{2R}^{\infty}(2g_{11} + g_{01})S^2\,dS. \end{aligned} \quad (72)$$

The functions g_{01} and g_{11} can be determined by solving the two sphere problems using the boundary conditions for P_{nm} as given by (37) [or (53)] and for the two extreme values of ρ^*, the detailed calculations give

$$C_a = 1 + 2.76\beta, \quad C_b = 1 + 2.11\beta,$$
$$C_d^r = 1 + 3.91\beta, \quad \rho^* = 0, \quad (73)$$

$$C_a = 1 + 3.32\beta, \quad C_b = 1 + 2.28\beta,$$
$$C_d^r = 1 + 5.94\beta, \quad \rho^* \simeq \infty. \quad (74)$$

As explained in the previous section, in these calculations we have assumed that the Stokes layers of the two particles do not overlap. Although this is incorrect for separation distances given by $S - 2R = O(\Omega R)$, it can be shown that the error associated with this approximation is smaller than $O(\Omega^2)$. Indeed, the integrand in (72) is affected by an amount smaller than $O(\Omega)$ when the Stokes layers of the two particles overlap and this incorrect estimate is used only for distances of $O(\Omega R)$.

The result for C can be expressed as

$$\begin{aligned} C &= 1 + 3\beta C_{a1} + 9\Omega(1 + 2\beta C_{b1}) + 9\Omega^2 \\ &\quad \times(1 + 5\beta C_{d1}^r) + O(\Omega^3, \beta^2) \end{aligned} \quad (75)$$

so that C_{a1}, C_{b1}, and C_{d1}^r are all unity for periodic arrays.

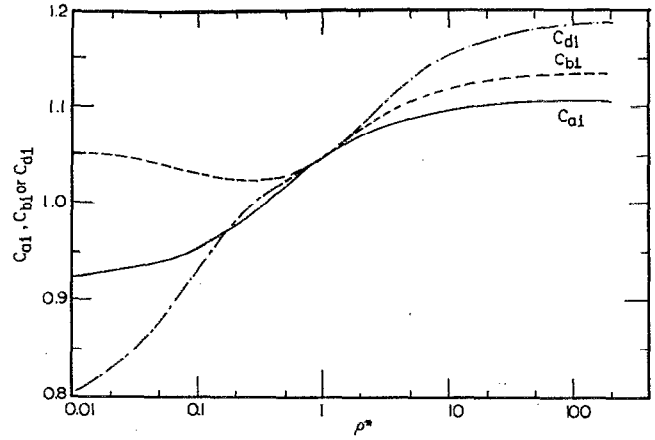

FIG. 1. The $O(\beta)$ coefficients [cf. (75)] in C_a, C_b, and C_d^r as functions of the nondimensional density ρ^* of particles. Here, β denotes the particle concentration by volume.

These coefficients for well-stirred random arrays as functions of ρ^* are shown in Fig. 1.

The analysis for dilute random arrays of bubbles free of surface-active impurities is presented in Sangani[1] and the result is given by (6). The coefficients of $O(\beta)$ in this case change very little as σ^* is varied from infinity to about 0.15. Below this value, large fluctuations appear owing to shape-dependent resonances. In terms of C, (6) for $\sigma^* = \infty$ can be written as

$$C_a = 1 + 2.76\beta, \quad C_d = 1 + 2.11\beta \quad (\sigma^* = \infty). \quad (76)$$

As mentioned earlier, C_d for impurities-free bubbles with $\sigma^* = \infty$ equals C_b for rigid particles with $\rho^* = 0$ and thus it is not surprising that the $O(\beta)$ coefficients in (73) and (76) are identical.

C. Velocity variance in dilute random arrays

In the situation envisaged here, the bubbles execute steady oscillatory motions around a fixed center. The amplitude and direction of these oscillations depend on the arrangement of the other bubbles in each particular realization and are therefore different for each bubble in general. It is therefore interesting to calculate the variance in the amplitude of the velocity of the bubbles from its mean. For dilute random arrays, this quantity can be estimated from pairwise interactions. The presence of a second particle situated at a separation vector $\mathbf{S}$ from the test particle placed at the origin changes the velocity of the latter by

$$\begin{aligned} \hat{\mathbf{v}}^*(\mathbf{O}|\mathbf{S}) - 3/(1 + 2\rho^*)\mathbf{G} &= g_{11}^*\mathbf{G} + (g_{01}^* - g_{11}^*) \\ &\quad \times[(\mathbf{G}\cdot\mathbf{SS})/S^2], \end{aligned} \quad (77)$$

where

$$g_{01}^* = g_{01} + 6(1-\rho^*)R^3/[(1 + 2\rho^*)^2 S^3]$$

and

$$g_{11}^* = g_{11} - 3(1-\rho^*)R^3/[(1 + 2\rho^*)^2 S^3]$$

are scalar functions of S/R including the $O[(R/S)^3]$ reflec-

tion in the two-particle interaction problem. Now, variance can be estimated to $O(\beta)$ from

$$\mathrm{Var} = \frac{\langle \hat{\mathbf{v}}\cdot\hat{\mathbf{v}}\rangle - \langle \hat{v}\rangle^2}{\langle \hat{v}\rangle^2} = \int_{S>2R} |g_{11}^* \mathbf{G} + (g_{01}^* - g_{11}^*)\mathbf{G}\cdot\mathbf{SS}/S^2|^2 P(\mathbf{S}|\mathbf{O})\,dV, \tag{78}$$

where the vertical bars denote the magnitude of the enclosed vector and the mean amplitude of the bubble velocity is approximated by its $O(\beta^0)$ estimate corresponding to the velocity of an isolated particle. For well-stirred random arrays, the above expression for the variance simplifies to

$$\mathrm{Var} = \beta \frac{(1+2\rho^*)^2}{9R^3} \int_{2R}^{\infty} (2g_{11}^{*2} + g_{01}^{*2}) S^2\,dS + O(\beta^2). \tag{79}$$

Detailed numerical calculations then yield

$$\mathrm{Var} = \begin{cases} 0.275\beta + O(\beta^2,\Omega), & \rho^* = 0, \\ 0.059\beta + O(\beta^2,\Omega), & \rho^* = \infty. \end{cases} \tag{80}$$

It is interesting to note that the contribution from the leading $O(R/S)^3$ terms in g_{11}^* and g_{01}^* to the $O(\beta)$ coefficient equals $(1-\rho^*)^2/[4(1+2\rho^*)^2]$, or 1/4 and 1/24 for ρ^* equal to 0 and ∞. The contribution from higher reflections is thus rather small in magnitude. It should also be noted that, while the mean velocity of the particles approaches zero as $\rho^* \to \infty$, the variance defined above remains finite because both the numerator and the denominator of (78) tend to zero at the same rate.

IV. ADDED MASS AND EFFECTIVE CONDUCTIVITY

There have been attempts in the literature to relate the added mass coefficient C_a in the inviscid case to the effective conductivity of a composite material consisting of a matrix containing inclusions with a different thermal (or electrical) conductivity.[1,4,16] While the calculation of both quantities requires the solution of the Laplace equation, the boundary conditions in the two problems are, in general, different. In this section, we study this issue and we prove that, although no universal relationship exists in general, there are some special situations for which an exact connection can be established. The first one, as noted by Biesheuvel and Spoelstra,[4] is when all the particles have equal velocities. In a dispersion this would either occur in a periodic array or in the limit in which the density of the particles is very large compared with that of the suspending fluid. Both cases, if for different reasons, are somewhat artificial for the application of present concern. Another case is that of small-amplitude oscillatory flow around bubbles with vanishingly small surface tension.

Consider the steady temperature field in a system consisting of a homogeneous matrix containing equal spherical inclusions of a different material. This temperature field satisfies the Laplace equation and can therefore be written in a manner analogous to (42) as

$$T(\mathbf{x}) = \mathbf{G}_T\cdot\mathbf{x} + \sum_{\alpha=1}^{N} \sum_{n=1}^{\infty} \sum_{m=0}^{m=n} 2^{m-1}\,\partial_1^{n-m} \times (B_{nm}^{\alpha}\Delta_m + \tilde{B}_{nm}^{\alpha}\tilde{\Delta}_m) S_1(\mathbf{x}-\mathbf{x}^{\alpha}), \tag{81}$$

where $\mathbf{G}_T$ is the average temperature gradient. Similarly, near the surface of a particle α, a representation analogous to (20) is available

$$T = \sum_{n=0}^{\infty} \sum_{m=0}^{n} [T_{nm}^{\alpha}(r)\cos m\phi + \tilde{T}_{nm}^{\alpha}(r)\sin m\phi] P_n^m(\cos\theta), \tag{82}$$

with T_{nm}^{α} and $\tilde{T}_{nm}^{\alpha}$ having the form (21), e.g.,

$$T_{nm}^{\alpha} = F_{nm}^{\alpha} r^n + H_{nm}^{\alpha} r^{-n-1}. \tag{83}$$

It is readily shown that the continuity of temperature and heat fluxes at the surface $r = R$ of the generic inclusion requires

$$F_{nm}^{\alpha} R^n + \tau_n H_{nm}^{\alpha} R^{-n-1} = 0, \tag{84}$$

with

$$\tau_n = (n\kappa + n + 1)/(\kappa - 1)n, \tag{85}$$

and $\kappa = k_d/k_c$ the ratio of the conductivities of the disperse and continuous phases. As before, all the coefficients B_{nm}^{α}, $\tilde{B}_{nm}^{\alpha}$, F_{nm}^{α}, and H_{nm}^{α} are linearly related and, in particular, a relation similar to (46) holds, namely

$$F_{10}^{\alpha} = (\partial_1 T^{(r)})_{\mathbf{x}=\mathbf{x}^{\alpha}}, \tag{86}$$

with $T^{(r)}$ the regular part of T defined as in (47).

The dimensionless effective conductivity $k^* = k_{\mathrm{eff}}/k_c$ can be obtained from the coefficients H_{10}^{α} according to[17]

$$k^*(\kappa) = 1 - 3\beta\langle H_{10}\rangle R^{-3}, \quad \langle H_{10}\rangle \equiv \frac{1}{N}\sum_{\alpha} H_{10}^{\alpha}, \tag{87}$$

in which, due to the linearity and isotropy of the problem, the H_{10}^{α} are evaluated with a mean temperature gradient of unit magnitude in the x_1 direction, $(\mathbf{G}_T)_i = \delta_{i1}$.

Let us now turn to the flow problem. If the particles' law of motion $\langle \hat{\mathbf{F}}\rangle = i\omega\rho_b v_b \langle \hat{\mathbf{v}}\rangle$ is substituted into the expression (9), we find

$$(\rho^* + \tfrac{1}{2}C_a)\langle \hat{\mathbf{v}}\rangle = (1 + \tfrac{1}{2}C_a)\langle \hat{\mathbf{u}}_m\rangle, \tag{88}$$

or, from (51),

$$[\rho^* + \tfrac{1}{2}C_a - \beta(1-\rho^*)(1+\tfrac{1}{2}C_a)]\langle \hat{\mathbf{v}}\rangle = (1+\tfrac{1}{2}C_a)\mathbf{G}. \tag{89}$$

Furthermore, with the neglect of viscous effects, we have from (38)

$$\hat{v}_1^{\alpha} = 3E_{10}^{\alpha} R^{-3}/(1-\rho^*), \tag{90}$$

so that, for $G_i = -\delta_{i1}$ [where the minus sign is introduced to compensate for the difference between the first terms in the right-hand sides of (42) and (81)], (89) gives

$$\left[\frac{\rho^* + \tfrac{1}{2}C_a}{1-\rho^*} - \beta\left(1 + \frac{1}{2}C_a\right)\right] 3R^{-3}\langle E_{10}\rangle = -\left(1 + \frac{1}{2}C_a\right). \tag{91}$$

It is clear that, if a connection between $\langle E_{10}\rangle$ and $\langle H_{10}\rangle$ can

be established, comparison of (87) and (91) will lead to a relation between k^* and C_a.

We consider the case of rigid particles first. Upon application of the boundary conditions (35) and (37), the following relation between the coefficients C^{α}_{nm} and E^{α}_{nm} appearing in the expansion (21) of P^{α}_{nm} is found

$$C^{\alpha}_{nm}R^{n} + \tau'_n E^{\alpha}_{nm} R^{-n-1} = 0, \tag{92}$$

where

$$\tau'_1 = (1+2\rho^*)/(1-\rho^*),$$
$$\tau'_n = -(n+1)/n, \quad n \geq 2. \tag{93}$$

For $\kappa = 0$, $\tau'_n = \tau_n$ for all $n \geq 2$. In addition, for $\rho^* \to \infty$ (i.e., for particles much heavier than the suspending fluid), also $\tau'_1 \to \tau_1$ so that, in this limit, $\tau'_n = \tau_n$ for all n's and $E^{\alpha}_{10} = H^{\alpha}_{10}$. Hence, from (87) and (91), we find

$$\left[1+\beta\left(1+\frac{1}{2}C_a\right)\right]\frac{1-k^*}{\beta} = 1+\frac{1}{2}C_a, \tag{94}$$

from which

$$C_a(\rho^* \to \infty) = 2\{[1-k^*(0)]/\beta k^*(0) - 1\}. \tag{95}$$

This relationship can readily be verified for the case of dilute random arrays, for which Jeffrey[12] obtained

$$k^*(0) = 1 - \tfrac{3}{2}\beta + 0.588\beta^2 + O(\beta^3). \tag{96}$$

Upon substitution into (95), one finds

$$C_a(\rho^* \to \infty) = 1 + 3.324\beta + O(\beta^2), \tag{97}$$

in agreement with (13) and (74).

It is rather remarkable that Eq. (95) also holds for periodic arrays irrespective of the value of ρ^*. This result rests on the fact that, in the periodic case, the coefficients B^{α}_{nm} and $\tilde{B}^{\alpha}_{nm}$ are all proportional to B^{α}_{10}, which is itself proportional to H^{α}_{10} (Ref. 9). The proof of this property requires the use of Eqs. (84) with $n \geq 2$. From (86), one can then write

$$F^{\alpha}_{10} = 1 + \eta H^{\alpha}_{10} R^{-3}, \tag{98}$$

with the specific expression of the proportionality constant η immaterial for the present purposes. A parallel argument can be carried through for the flow problem to obtain

$$C^{\alpha}_{10} = 1 + \eta E^{\alpha}_{10} R^{-3}. \tag{99}$$

The crucial point here is that, since $\tau_n = \tau'_n$ for $n \geq 2$ and $\kappa = 0$, the two constants η in (98) and (99) are identical. From (84) with $\kappa = 0$ and (92), we also have

$$C^{\alpha}_{10} = [(2\rho^*+1)/(\rho^*-1)]E^{\alpha}_{10}R^{-3},$$
$$F^{\alpha}_{10} = 2H^{\alpha}_{10}R^{-3}, \tag{100}$$

so that

$$R^{-3}E^{\alpha}_{10} = (\rho^*-1)/[2\rho^*+1-\eta(\rho^*-1)],$$
$$R^{-3}H^{\alpha}_{10} = 1/(2-\eta). \tag{101}$$

Upon substitution of these expressions into (87) and (91), one finds

$$C_a = 2[(1+3\beta+\eta)/(2-3\beta-\eta)],$$
$$k^* = 1 - 3\beta/(2-\eta), \tag{102}$$

and, upon elimination of η, the relationship (95) is found, now independently of the value of ρ^*.

We now turn to the other situation mentioned before, namely the small-amplitude oscillatory flow around massless bubbles with vanishing surface tension. In this case, the bubbles deform so as to maintain a constant pressure—and therefore also a constant potential—over their surface. Equation (40) can then be cast into the form (92) with

$$\tau'_n = [1-(n^2-1)(n+2)\sigma^*]/$$
$$[1+n(n-1)(n+2)\sigma^*], \tag{103}$$
$$n \geq 1.$$

Thus, when $\sigma^* = 0$ and $\kappa \to \infty$, once again we find $E^{\alpha}_{nm} = H^{\alpha}_{nm}$. Upon setting $\rho^* = 0$, we then obtain from (87) and (91)

$$C_a(\sigma^* = 0) = 2\{[k^*(\infty)-1]/\beta k^*(\infty) - 1\}^{-1}. \tag{104}$$

Again, for dilute random arrays, Jeffrey[12] obtained

$$k^*(\infty) = 1 + 3\beta + 4.51\beta^2 + O(\beta^3). \tag{105}$$

Upon substitution into (104), we then find

$$C_a(\sigma^* = 0) = 1 + 2.245\beta + O(\beta^2), \tag{106}$$

in agreement with the results obtained using (6) in (11). While this limit case is fairly realistic for relatively large bubbles, it should be remarked that the limit $\sigma^* = 0$ is not approached smoothly as λ_v goes through an infinite number of discontinuities as shown in Ref. 1.

V. NUMERICAL RESULTS FOR NONDILUTE MIXTURES

A. Simulation of random arrays and convergence tests

To obtain estimates of λ_v or, equivalently, C, we generate a random configuration of N bubbles within a unit cell making sure that there is no overlap between any of the bubbles in the cell nor with those in the adjoining cells that are its exact replicas. Figure 2 shows the radial distribution func-

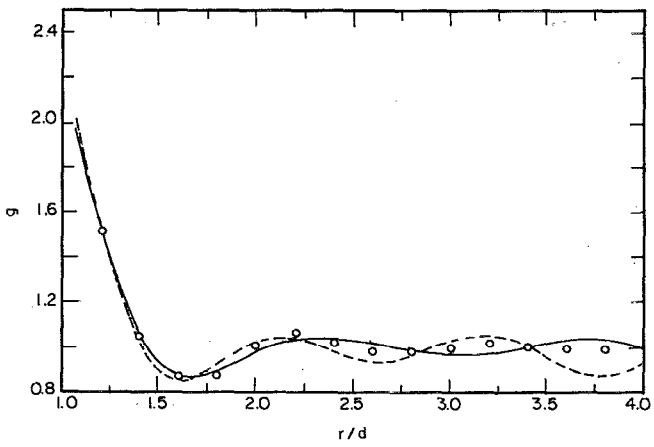

FIG. 2. The radial distribution function g for random arrays with a particle volume concentration $\beta = 0.3$ simulated with $N = 16$ particles (dashed curve) and $N = 32$ (solid curve). The open circles are the corresponding results from the Percus–Yevick equation as obtained by Throop and Bearman (Ref. 17). Here, r is the distance from the test particle, d is the diameter of the particles, and g is normalized such that it approaches unity for large r.

tion for a few selected configurations with $\beta = 0.3$ and N equal to 16 and 32. The corresponding cell sizes are, respectively, 3.0 and 3.8 times the diameter of the bubbles. The numerical solution of the well-known Percus–Yevick equation for the pair distribution function of a random distribution of nonoverlapping particles as obtained by Throop and Bearman[18] is shown in Fig. 2 by the open circles. Their results are approximated quite well with only 16 or 32 particles, particularly for the smaller separation distances, which are likely to be the most important ones in determining the behavior of nondilute suspensions.

As mentioned earlier, the randomly generated configurations of bubbles are not isotropic in general and therefore λ_v is actually a tensor of rank two. For each configuration, the nine components of λ_v were determined for a mean mixture acceleration or, more precisely, $\mathbf{G}$, in three mutually perpendicular directions. The off-diagonal elements of the tensor were generally found to be much smaller (typically two orders of magnitude) than the diagonal elements and a mean of the three diagonal components was taken as the estimate of a scalar value of λ_v applicable to isotropic configurations. The results for λ_v thus obtained were checked for convergence for various values of N and of the highest order N_S of singularity retained in Eq. (42). The total number of unknowns used in the computations is given by $N_s(N_s + 2)N$. The convergence of the numerical results for a random configuration with $N = 16$, $\rho^* = 0$, and $\beta = 0.3$ is illustrated in Fig. 3, which shows the percent deviation of λ_a, λ_b, and λ_d from their converged value as a function of N_S. These coefficients are defined by

$$\lambda_v = \lambda_a + \Omega\lambda_b + \Omega^2\lambda_d. \tag{107}$$

As shown in Fig. 3, the results have virtually converged for N_s of about 7. The percent deviations from the converged values are quite low (a few percent) even for $N_s = 1$. All subsequent calculations were therefore carried out with $N_s = 5$ (where the deviations are less than 0.1%), except for some calculations for higher β values for which $N_s = 6$ was used.

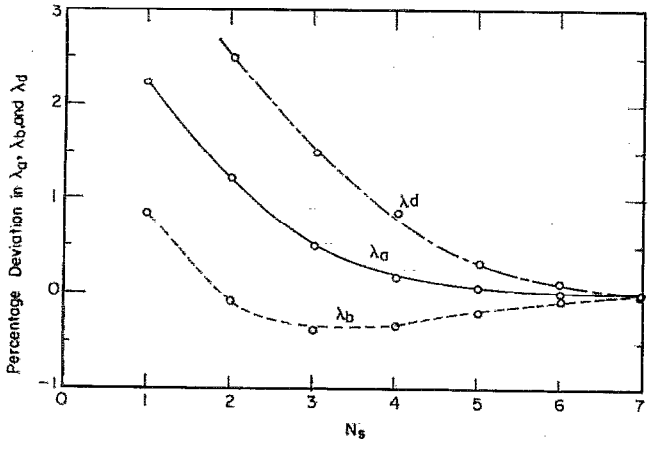

FIG. 3. Convergence of the numerical results for λ_a, λ_b, and λ_d [cf. (107)] as a function of the order N_s of singularities retained in the expansion (42). The percentage deviation for each quantity is calculated from its value at $N_s = 7$. Here, $\beta = 0.3$, $N = 16$, and $\rho^* = 0$. The total number of unknowns used in the computation is $N_s(N_s + 2)N$.

B. Details of the computations

The computation consists of first determining the elements of a square matrix of size $N N_s(N_s + 2)$, which are related to various derivatives of S_1 [cf. (42)], for all the separation vectors between the $N(N-1)/2$ pairs of bubbles. The derivatives are evaluated by using an Ewald summation representation of S_1 as given by Hasimoto[10] together with an improvement over the method described in Sangani and Behl[19] (see the Appendix). The total CPU time for the determination of all of the nine components of the tensors λ_a, λ_b, and λ_d on the supercomputer at Cornell Theory Center with $N_s = 5$ and $N = 16$ (a total of 560 unknowns) was about 28 sec, of which 11 were used in the vectorized mode. The calculation of the multiparticle interaction matrix elements required about 12.7 sec, while solving a system of 3×560 linear equations required about 5 sec. (Here, the factor 3 corresponds to the calculation of the components of λ_v in correspondence of the three mutually perpendicular directions of $\mathbf{G}$.) This system of equations must be solved successively three times corresponding to the calculation of $O(\Omega^0)$, $O(\Omega^1)$, and $O(\Omega^2)$, making the overall time of $12.7 + 3 \times 5 \simeq 28$ sec. More specifically, the system of equations to be solved can be written in the form $\mathbf{B}\cdot\mathbf{X} = \mathbf{Y}$, where $\mathbf{B}$ is the aforementioned multiparticle interaction matrix, $\mathbf{X}$ is the unknown 3×560 matrix of A_{nm} and $\tilde{A}_{nm}$ [cf. (42)], and $\mathbf{Y}$ is a 3×560 matrix determined from the boundary conditions on the bubbles. Since we are expanding the unknowns A_{nm}, etc., in powers of Ω up to $O(\Omega^2)$, we must solve these systems of equations separately three times. The computations of A^0_{nm} and $\tilde{A}^0_{nm}$ are used in determining the elements of $\mathbf{Y}^1$ and those of A^1_{nm}, $\tilde{A}^1_{nm}$, etc., in determining the elements of $\mathbf{Y}^2$. The matrix $\mathbf{B}$ remains unchanged.

In view of the rather modest computational requirements, we did not utilize the highly efficient software for solving systems of linear equations that are now available on supercomputer libraries, but we estimate that the present computational time can be reduced further, roughly by a factor of 2, by taking advantage of such software and by making the vectorization code for determining the coefficients of the matrix $\mathbf{B}$ more efficient. (Of the 12.7 sec used in computing the coefficients of $\mathbf{B}$, only 2 sec were utilized in the vector mode.) Finally, we note that the CPU time in the calculation scheme presented here will roughly increase as N^2 for larger N.

C. Numerical results

Figure 4 shows λ_a as a function of N for $\rho^* = 0$ and $\beta = 0.3$ as determined by averaging over 8–10 configurations. The computed values of the mean for $N = 8$, 16, and 32 are shown by circles. These mean values are, of course, related to the mean of $\hat{v}$ for each bubble; the standard deviation of $\hat{v}$ from its mean is shown by vertical bars. More pre-

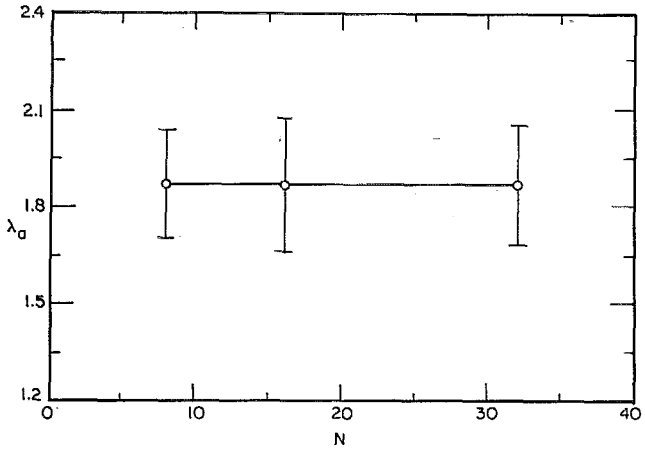

FIG. 4. The leading-order term λ_a of the velocity ratio λ_n [cf. (1) and (107)] as a function of the number of particles in the basic cell N. Each vertical bar represents two standard deviations of the amplitude of the bubble velocity from its mean [cf. (108)]. Here, the particles are massless ($\rho^* = 0$) and their concentration by volume is $\beta = 0.3$.

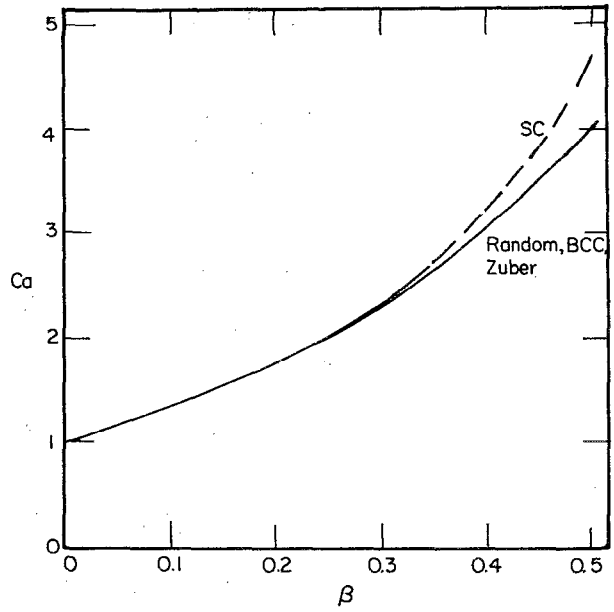

FIG. 5. The added mass coefficient C_a as a function of the particle volume concentration β for $\rho^* = 0$. The results for body-centered cubic arrays, random arrays, and the cell theory approximation of Zuber (Ref. 10) are all represented by the solid curve. The dashed curve is for simple cubic arrays.

cisely, the vertical bars are two standard deviations with the standard deviation (s.d.) defined by

$$(\text{s.d.})^2 \equiv \text{Var}\cdot\langle\hat{v}\rangle^2 = N^{-1}\sum_{\alpha=1}^{N}(\hat{\mathbf{v}}^\alpha\cdot\hat{\mathbf{v}}^\alpha) - \langle\hat{\mathbf{v}}\rangle\cdot\langle\hat{\mathbf{v}}\rangle. \quad (108)$$

It should be noted that this standard deviation is primarily a function of β for random arrays and should only weakly depend on N. Since the results for λ_a and its standard deviation change very little with N, all the subsequent results were made with $N = 16$.

Figure 5 shows C_a for $\rho^* = 0$ as a function of β. The results for a random array are obtained by averaging over 12–15 configurations with $N = 16$, with each configuration providing three estimates of C_a corresponding to the three mutually perpendicular directions of $\mathbf{G}$. The results for the body-centered cubic array are virtually indistinguishable from those for the random arrays. For sufficiently small $\beta(\simeq 0.03)$, the coefficient of $O(\beta)$ in C_a as determined from the numerical calculations for periodic arrays is slightly greater than that for random arrays, in agreement with our dilute-array theoretical results described in the previous section. The difference in the values of C_a for the two arrays, however, remains very small for all values of β up to 0.5. (At small β values, C_a for the body-centered cubic array is slightly larger whereas at larger β values the random arrays have a slightly larger value.) Furthermore, it is interesting to note that the analytical formula (63) for C_a for dilute periodic arrays also remains within 2% of the C_a values for random arrays for β up to 0.5. Since this formula agrees with the well-known estimate given by Zuber[11] using a cell approximation, we conclude that this approximation is excellent. The difference between C_a for simple cubic and random arrays is also relatively small, so that we may conclude that C_a is a very insensitive function of the geometry of the array (at least for well-separated particle distributions).

The above calculations of C_a were based on $\rho^* = 0$. The dependence of C_a on ρ^* is also very weak, as shown in Fig. 6. For small β values ($\beta \simeq 0.03$), the C_a for random arrays with $\rho^* = \infty$ was found to be greater than that of a periodic array, and C_a for random arrays with $\rho^* = 0$ was found to be smaller than that of the periodic array, in accordance with our dilute theory analysis [cf. (62), (73), and (74)]. The difference in C_a values, however, remained small for larger β values. The difference between the C_a values for $\rho^* = 0$ and ∞ at $\beta = 0.3$ is less than 8% and that at $\beta = 0.5$ is even smaller, 2.5%. Since different values of ρ^* imply different relative velocity distributions among the bubbles, we con-

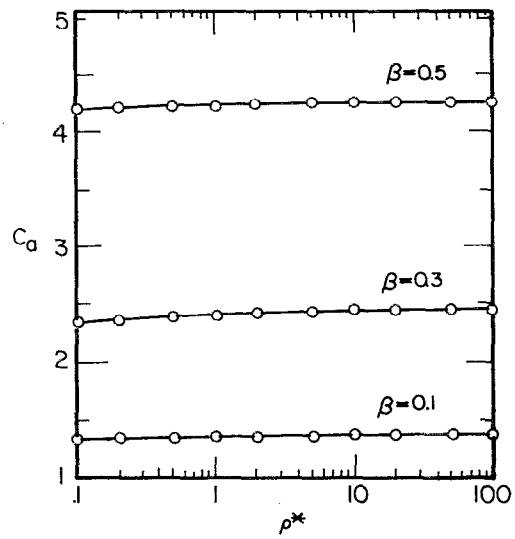

FIG. 6. The added mass coefficient C_a as a function of the density ratio ρ^*.

clude that C_a is a rather insensitive function of the velocity distribution as well.

The magnitude of the fluctuations in the velocity of the bubbles from its mean plays an important role in the stability of bubbly flows. Figure 7 shows the variance of this quantity [cf. (78)] as a function of β for random arrays with $\rho^* = 0$. These results have been obtained with $N = 16$ and are averaged over about 15 configurations for each β. Unlike the case of C_a, which exhibited only small variations among different configurations with the same β, deviations in the variance by as much as 50% among different configurations were found to be common. Hence, it is important to average over a sufficiently large number of configurations in order to obtain reliable estimates of variance. The expression for the variance of dilute random arrays derived in Sec. III [cf. (80)] was verified from the detailed numerical calculations with β equal to 0.01 and 0.02. At such small β values, the variations among different configurations is particularly large. In fact, we observed large fluctuations in the variance even with N as great as 80 (with $N_s = 1$ and 3). The calculations for the variance were carried out only up to $\beta = 0.5$. The dashed curve in Fig. 7 is an extrapolation based on the assumption that the variance will become zero for β close to 0.62.

The effect of surface tension on C_a and the variance for random arrays with $\beta = 0.3$ is shown in Fig. 8. There is very little variation in C_a or the variance as the nondimensional surface tension σ^* is decreased from ∞ to about 0.2. For smaller values of σ^*, C_a begins to increase slowly and there is a very rapid increase in the variance. In fact, the variance becomes comparable to unity by σ^* of about 0.12 so that the very notion of an average added mass coefficient of the distribution becomes meaningless. As mentioned in the Introduction, such large variations in the bubble velocities arise due to shape-dependent resonances in the pairwise interactions of bubbles.

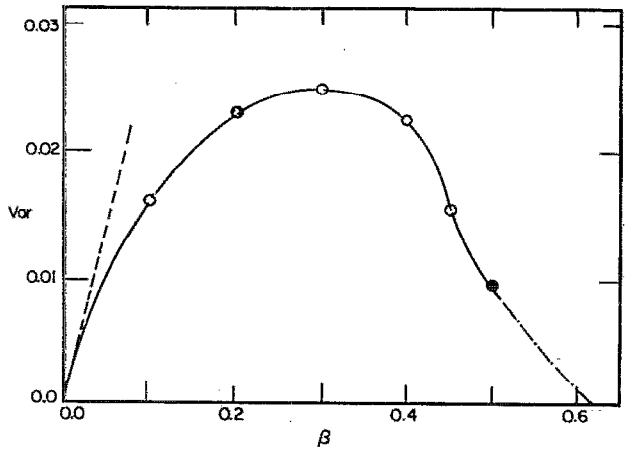

FIG. 7. The velocity variance [cf. (78)] as a function of β for massless particles ($\rho^* = 0$). The solid line represents the computed values, the dashed line shows the theoretical results for small β, and the dot-dashed curve is an extrapolation based on the assumption that the variance approaches zero as $\beta \to 0.62$.

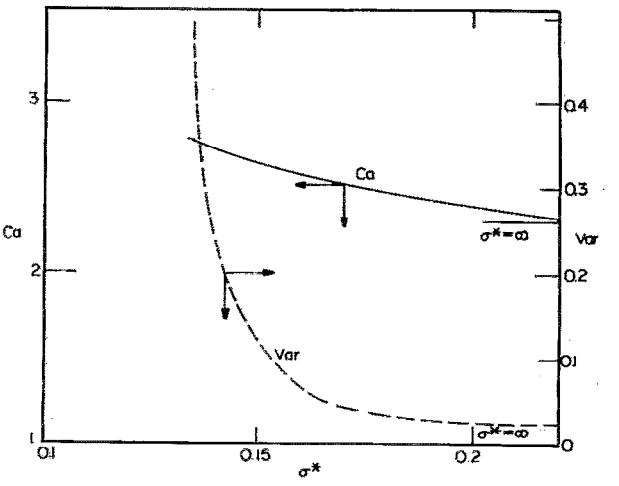

FIG. 8. The added mass coefficient and variance in the amplitude of the bubble velocity as a function of the nondimensional surface tension σ^* for impurities-free bubbles with $\beta = 0.3$.

The results for the Basset force coefficient C_b for rigid particles with $\rho^* = 0$ are shown in Fig. 9. In accordance with (73), the values for random arrays are slightly larger than for periodic arrays for small β. However, the difference between the body-centered cubic array and the random array is not great and, in fact, the formula $C_b = 1/(1-\beta)^2$ [cf. (62)] for dilute periodic arrays gives better than 10% accurate estimates for $\beta \leqslant 0.5$. For simple cubic arrays, C_b is

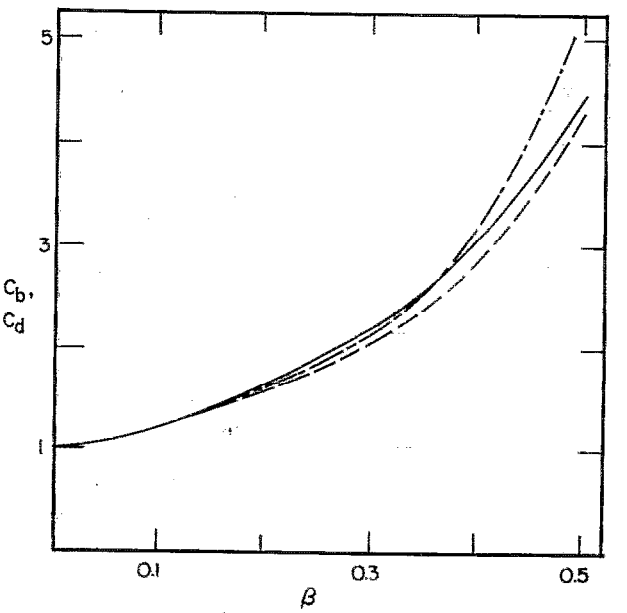

FIG. 9. The Basset force coefficient C_b as a function of β for massless particles ($\rho^* = 0$). The solid curve is for random arrays, the dashed curve is for the body-centered cubic array, and the dashed and dotted curve is for the simple cubic array. Note that these results for C_b also apply to the viscous drag coefficient of impurities-free bubbles with σ^* greater than about 0.2.

slightly lower than for random arrays at smaller β values and begins to increase more rapidly for $\beta > 0.4$. We note that the difference in C_b among all the arrays is rather small for β values of up to 0.4. The variation of C_b with ρ^* was also found to be very small. For example, the largest variation in C_b values, which occurs for $\beta = 0.5$ and $\rho^* = 0$ and ∞, was found to be less than 5%. Finally, it should be noted that the results for C_b with $\rho^* = 0$ also apply to the viscous drag coefficient C_d of impurities-free bubbles with σ^* greater than about 0.2.

The results for the viscous drag coefficient C_d^r of rigid particles with $\rho^* = 0$ are shown in Fig. 10. The C_d^r of random arrays is slightly lower than for periodic arrays for β less than about 0.03. (The difference, however, is too small to be seen in the figure.) For β greater than about 0.05, C_d^r for random arrays becomes greater than for simple and body-centered cubic arrays. Finally, C_d^r for the simple cubic array begins to increase more rapidly for β greater than about 0.35, beyond which point C_d^r for random arrays becomes smaller than for the simple cubic case. The estimate $C_d^r = (1 + 2\beta)/(1 - \beta)^3$ for dilute periodic arrays gives correct estimates within 10% for simple cubic arrays for $\beta \leqslant 0.3$ and for body-centered cubic arrays for $\beta \leqslant 0.45$.

VI. CONCLUSIONS

In summary, our detailed calculation of the coefficient of added mass C_a, Basset force C_b, and viscous drag C_d and C_d^r suggests these quantities to be relatively insensitive functions of the geometry of the array (at least for well-separated particle distributions), the density ratio ρ^*, and the surface tension parameter σ^* (provided the latter is larger than about 0.2). In particular, the simple estimates of these quantities for dilute periodic arrays given by Eqs. (61)–(64) in Sec. III can be used with a reasonable degree of accuracy.

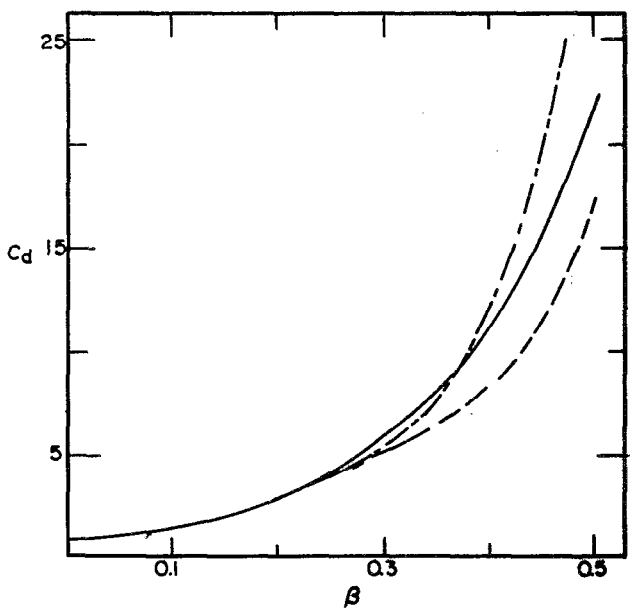

FIG. 10. The viscous drag coefficient C_d^r for rigid particles with $\rho^* = 0$ as a function of β. The solid curve is for random arrays, the dashed curve is for the body-centered cubic array, and the dashed and dotted curve is for the simple cubic array.

After the original submission of this paper, a paper by Felderhof was published in which the added mass and drag coefficients of suspensions of particles undergoing small-amplitude oscillatory motion are also studied.[20] Felderhof's expressions for C_a and C_d depend, in addition to the volume fraction, on a single parameter γ, which he evaluates analytically to order β for the case of dilute arrays by using the pairwise interaction theory. For the nondilute case, estimates of γ are obtained by relating it to two statistical parameters, the three-point correlation function ζ_2 introduced by Beran[21] and recently evaluated by Torquato and Lado[22] and Sangani and Yao,[9] and a constant s_2 related to the Kirkwood–Yvon integrals recently calculated by Cichocki and Felderhof.[23] With these estimates of ζ_2 and s_2, Felderhof calculates approximate values of C_a for $0 \leqslant \beta \leqslant 0.5$ and $0 \leqslant \rho^* < \infty$. His results for the $O(\beta)$ correction to C_a are in perfect agreement with our Fig. 1. The numerical results for nondilute arrays are also in good agreement. For example, at $\beta = 0.5$, the difference is 8%. This agreement, however, does not constitute a very stringent proof of the correctness of Felderhof's approximations since, as was mentioned earlier, even the simple cell model of Zuber (which amounts to taking $\zeta_2 = s_2 = 0$) also gives estimates of C_a within a few percentage points of our exact results.

Felderhof's results for the viscous drag coefficient, on the other hand, appear to be inconsistent with ours. Unfortunately he does not present many details and it is therefore difficult to determine the source of this discrepancy. As a matter of fact, we believe that it is unlikely that C_a and C_d can both depend on the single parameter γ. As our analysis shows, the presence of the Stokes layer around the surface of a particle affects the viscous pressure contribution on all the other spheres in the suspension and thus the determination of C_d is rather involved. Felderhof's paper does not mention this important effect and we believe that this might be the origin of the difference.

ACKNOWLEDGMENTS

This work has been supported by the Department of Energy, Office of Basic Energy Sciences, under Grants No. DE-FG02-89ER14043 and No. DE-FG02-90ER14136. A. S. also acknowledges support from the National Science Foundation under Grant No. CBT-8800451 and D. Z. Z. and A. P. under Grant No. CBT-8918144. The authors are also grateful for the use of the supercomputer facilities at the Cornell Theory Center.

APPENDIX: THE DERIVATIVES OF S_1

The function S_1 and its derivatives appearing in Eq. (42) are most efficiently evaluated by the use of the Ewald sum representation as given by Hashimoto,[9]

$$S_1(\mathbf{x}) = \zeta^{-1/2} \sum_{\mathbf{L}} \gamma\left(-\frac{1}{2}, \frac{\pi(\mathbf{x} - \mathbf{x}_\mathbf{L})^2}{\zeta}\right) - \frac{\zeta}{V} + \frac{\zeta}{V} \sum_{\mathbf{k} \neq 0} \Gamma^*(0, \pi\zeta k^2) \cos(2\pi \mathbf{k}\cdot\mathbf{x}), \quad \text{(A1)}$$

where V is the volume of the basic cell, $\mathbf{x}_L$ are the lattice vectors, $\mathbf{k}$ the vectors of the reciprocal lattice, and ζ is an arbitrary constant. Neither the value of S_1 nor those of its derivatives depend, of course, on any particular choice of this parameter. The value $\zeta = h^2$, h being the side of the basic cell, is found to be convenient for the numerical computations. In Eq. (A1), Γ^* is an incomplete gamma function defined by

$$\Gamma^*(\mu,x) = \int_1^\infty \exp(-x\xi)\xi^\mu \, d\xi. \tag{A2}$$

The above expression for S_1 may be differentiated in a manner similar to that given in Ref. 19 to obtain

$$\partial_1^{n-m}\Delta_m S_1 = \zeta^{-1/2} \sum_{\mathbf{L}} \sum_{s=0}^{[(n-m)/2]} \left(-\frac{\pi}{\zeta}\right)^{n-s} 2^{n-m-2s+1} \frac{(n-m)!}{s!(n-m-2s)!} \Gamma^*\left(n-s-\frac{1}{2}, \frac{\pi(\mathbf{x}-\mathbf{x}_L)^2}{\zeta}\right)$$
$$\times y_{1L}^{n-m-2s} R_L^m \cos m\phi_L - \frac{2\zeta}{V}\delta_{n0}\delta_{m0}$$
$$+ \frac{\zeta}{V} \sum_{\mathbf{k}\neq 0} 2^{1-m}(-2\pi)^n \cos\left[2\pi\left(\mathbf{k}\cdot\mathbf{x} + \frac{n}{4}\right)\right] \Gamma^*(0,\pi\zeta k^2) k_1^{n-m} K^m \cos m\Phi_k, \tag{A3}$$

where $[(n-m)/2]$ denotes the integral part of $(n-m)/2$ and y_{1L}, R_L, Φ_L, K, and Φ_k are defined by

$$y_{1L} = x_1 - x_{1L}, \quad R_L \cos\Phi_L = x_2 - x_{2L},$$
$$R_L \sin\Phi_L = x_3 - x_{3L}, \quad k_2 = K\cos\Phi_k, \tag{A4}$$
$$k_3 = K \sin\Phi_k.$$

The formula for differentiation according to the operator $\tilde{\Delta}_n$ is similar except that the cosine terms are replaced by sine terms. We have found that these relations are computationally more efficient than those used in Ref. 9.

With the use of the above expression, we can also determine more complicated derivatives of S_1. For example,

$$\Delta_m\Delta_n S_1 = \Delta_{m+n} S_1 + \partial_\xi^n \partial_\eta^n \Delta_{m-n} S_1 \quad \text{for } m > n$$
$$= \Delta_{m+n} S_1 + (-\tfrac{1}{4})^n (\partial_1^{2n} - n\partial_1^{2n-2}\nabla^2)\Delta_{m-n} S_1, \tag{A5}$$

where use has been made of the fact that $\partial_\xi \partial_\eta = \frac{1}{4}(\nabla^2 - \partial_1^2)$ and that $\nabla^4 S_1 = 0$.

[1] A. S. Sangani, J. Fluid Mech. **232**, 221 (1991).
[2] L. van Wijngaarden, J. Fluid Mech. **77**, 24 (1976).
[3] A. Biesheuvel and L. van Wijngaarden, J. Fluid Mech. **148**, 301 (1984).
[4] A. Biesheuvel and S. Spoelstra, Int. J. Multiphase Flow **15**, 911 (1989).
[5] M. J. Lighthill, *An Informal Introduction to Theoretical Fluid Mechanics* (Oxford U.P., Oxford, 1986).
[6] A. S. Sangani, H. S. Kim, A. Prosperetti, and D. Z. Zhang, *Proceedings of the Eighth Symposium on Energy Engineering Sciences, Micro/Macro Studies of Multiphase Media*, edited by D. Frederick (Argonne National Laboratory, Argonne, IL, 1990), Rep. No. CONF-9005183, p. 144.
[7] L. D. Landau and E. M. Lifshitz, *Fluid Mechanics. Course of Theoretical Physics* (Pergamon, Oxford, 1959), Vol. 6.
[8] S. Kim and W. B. Russel, J. Fluid Mech. **154**, 253 (1985).
[9] A. S. Sangani and C. Yao, J. Appl. Phys. **63**, 1334 (1988).
[10] H. Hasimoto, J. Fluid Mech. **5**, 317 (1959).
[11] N. Zuber, Chem. Eng. Sci. **19**, 897 (1964).
[12] D. J. Jeffrey, Proc. R. Soc. London Ser. A **335**, 355 (1973).
[13] G. K. Batchelor, Annu. Rev. Fluid Mech. **6**, 227 (1974).
[14] E. J. Hinch, J. Fluid Mech. **83**, 695 (1977).
[15] A. Acrivos and E. Y. Chang, *Physics and Chemistry of Porous Media*, AIP Conf. Proc. No. 154, edited by J. R. Banavar, J. Koplik, and K. W. Winkler (AIP, New York, 1986), p. 129.
[16] G. Wallis, in *Multiphase Science and Technology*, edited by G. F. Hewitt, J. M Delhaye, and N. Zuber (Hemisphere, New York, 1990), Vol. 5, p. 270.
[17] R. C. McPhedran and D. R. McKenzie, Proc. R. Soc. London Ser. A **359**, 45 (1978).
[18] G. J. Throop and R. J. Bearman, J. Chem. Phys. **42**, 2408 (1965).
[19] A. S. Sangani and S. Behl, Phys. Fluids A **1**, 17 (1989).
[20] B. U. Felderhof, J. Fluid Mech. **225**, 177 (1991).
[21] M. Beran, Nuovo Cimento **38**, 771 (1965).
[22] S. Torquato and F. Lado, Phys. Rev. B **33**, 6428 (1986).
[23] B. Cichocki and B. U. Felderhof, J. Stat. Phys. **53**, 499 (1988).